

*Stratigraphy of the Tuffs from
Borehole 49-2-700-1 at
Technical Area 49,
Los Alamos National Laboratory,
New Mexico*



Produced by Risk Reduction and Environmental Stewardship Division

Cover photo shows a modified Foremost DR-24 dual-rotary drill rig. The DR-24 is one of several drill-rig types being used for drilling, well installation, and well development in support of the Los Alamos National Laboratory Hydrogeologic Workplan. The Hydrogeologic Workplan is jointly funded by the Environmental Restoration Project and Defense Programs to characterize groundwater flow beneath the 43-square-mile area of the Laboratory and to assess the impact of Laboratory activities on groundwater quality. The centerpiece of the Hydrogeologic Workplan is the installation of up to 32 deep wells in the regional aquifer.

An Affirmative Action/Equal Opportunity Employer

This report was prepared as an account of work sponsored by an agency of the United States Government. Neither The Regents of the University of California, the United States Government nor any agency thereof, nor any of their employees, makes any warranty, express or implied, or assumes any legal liability or responsibility for the accuracy, completeness, or usefulness of any information, apparatus, product, or process disclosed, or represents that its use would not infringe privately owned rights. Reference herein to any specific commercial product, process, or service by trade name, trademark, manufacturer, or otherwise, does not necessarily constitute or imply its endorsement, recommendation, or favoring by The Regents of the University of California, the United States Government, or any agency thereof. The views and opinions of authors expressed herein do not necessarily state or reflect those of The Regents of the University of California, the United States Government, or any agency thereof. Los Alamos National Laboratory strongly supports academic freedom and a researcher's right to publish; as an institution, however, the Laboratory does not endorse the viewpoint of a publication or guarantee its technical correctness.

*Stratigraphy of the Tuffs from Borehole 49-2-700-1 at
Technical Area 49, Los Alamos National Laboratory,
New Mexico*

*J. A. Stimac**
D. E. Broxton
E. C. Kluk
S. J. Chipera
*J. R. Budahn***

** Philippine Geothermal, Inc.*

***US Geological Survey, Denver, Colorado*



Table of Contents

ABSTRACT	1
1.0 INTRODUCTION	2
2.0 METHODS.....	3
3.0 RESULTS AND DISCUSSION	5
3.1 Lithologies.....	5
3.2 Moisture Distribution	7
3.3 Fractures and Alteration.....	8
3.4 Chemistry.....	8
3.5 Mineralogy.....	8
4.0 ACKNOWLEDGEMENTS	12
5.0 REFERENCES.....	12

APPENDIX A. BULK-ROCK CHEMICAL COMPOSITIONS FOR BOREHOLE 49-2-700-1

APPENDIX B. INAA RESULTS FOR BOREHOLE 49-2-700-1

APPENDIX C. BULK-TUFF MINERALOGY FOR BOREHOLE 49-2-700-1

**STRATIGRAPHY OF TUFFS FROM BOREHOLE 49-2-700-1 AT TECHNICAL AREA 49,
LOS ALAMOS NATIONAL LABORATORY, NEW MEXICO**

by

J.A. Stimac, D.E. Broxton, E.C. Kluk, S.J. Chipera, J.R. Budahn

ABSTRACT

This report presents the stratigraphy of tuffs encountered in borehole 49-2-700-1 located at TA-49. The primary methods of investigation included hand-sample observation (hand lens and binocular microscope), supplemented by limited scanning electron microscopy. Selected samples were analyzed by X-ray fluorescence (XRF) and instrumental neutron activation analyses (INAA) for major and trace element composition. Additional samples were analyzed by quantitative X-ray diffraction (QXRD) to determine mineralogy. This investigation provides necessary data to develop conceptual models for the hydrogeology of the site, evaluate potential transport pathways and processes, and provide a stratigraphic framework for numerical models evaluating migration of water and contaminants.

Geologic field observations in adjacent canyons helped verify the thickness and character of the stratigraphic units in the upper portion of the borehole. The exposed bedrock stratigraphic sequence in Water Canyon is restricted to units of the Tshirege Member of the Bandelier Tuff. The Tshirege Member is a multiple-flow, ash-flow sheet that forms a series of step-like vertical cliffs and sloping ledges along canyon walls. Canyon exposures immediately north of the borehole consist of, in ascending order, Qbt 1g, Qbt 1v, Qbt 2, Qbt 3, and Qbt 4 of the Tshirege Member.

Because the borehole extended beneath the level of adjacent canyon floors, a number of unexposed units were encountered, including, in descending order, the Tsankawi Pumice Bed, tephra and volcanoclastic sediments of the Cerro Toledo interval, and the Otowi Member of the Bandelier Tuff. The borehole bottomed in the upper part of Otowi Member.

The Otowi Member and units Qbt 1g through Qbt 3 of the Tshirege Member are high-silica rhyolites (77% SiO₂, on a volatile-free basis). Qbt 4 of the Tshirege Member is significantly less silicic (74% SiO₂) than underlying tuffs. Major element abundances for these units show relatively little variability (except for Qbt 4), but both the Otowi and Tshirege Members are compositionally zoned with respect to their trace elements.

The pre-eruptive phenocryst assemblage of both the Tshirege and Otowi Members is dominated by alkali feldspar and quartz. The post-eruptive mineralogy is dominated by volcanic glass in the Otowi Member, in the Cerro Toledo interval, and in Qbt 1g of the Tshirege Member. Units Qbt 1v, Qbt 2, Qbt 3, and Qbt 4 of the Tshirege Member are devitrified and vapor-phase altered, and their post-eruptive mineralogy is dominated by feldspar + quartz ± cristobalite ± tridymite ± smectite ± hematite.

Examination of moisture contents suggests some lithologic control. The most prominent features of the moisture data are abrupt increases in moisture content at the transition from glassy (Qbt 1g) to devitrified (Qbt 1v) Tshirege Member and at the Tsankawi Pumice Bed.

1.0 INTRODUCTION

This investigation describes the stratigraphy, lithology, mineralogy, and chemistry of the tuffs that underlie TA-49, based on detailed logging of core from borehole 49-2-700-1. TA-49 is located in the south-central portion of Los Alamos National Laboratory (LANL), north of State Highway 4 (Figure 1). This study was part of work that the Environmental Restoration (ER) Project performed at TA-49.

Drilling of borehole 49-2-700-1 began on November 17, 1993, and was completed January 25, 1994. The borehole was drilled by air-rotary methods and achieved its target depth of 700 ft. Continuous core was collected using a 3.25-in. diameter rock barrel from 0-50 ft and a 2.4-in. diameter rock barrel from 50-700 ft. ODEX casing (10-in. inner diameter [ID]) was set in the hole from 0-50 ft and grouted. From 10-700 ft, ODEX casing telescopes to 8-in. ID. The core was stored at the ER Sample Management Facility.

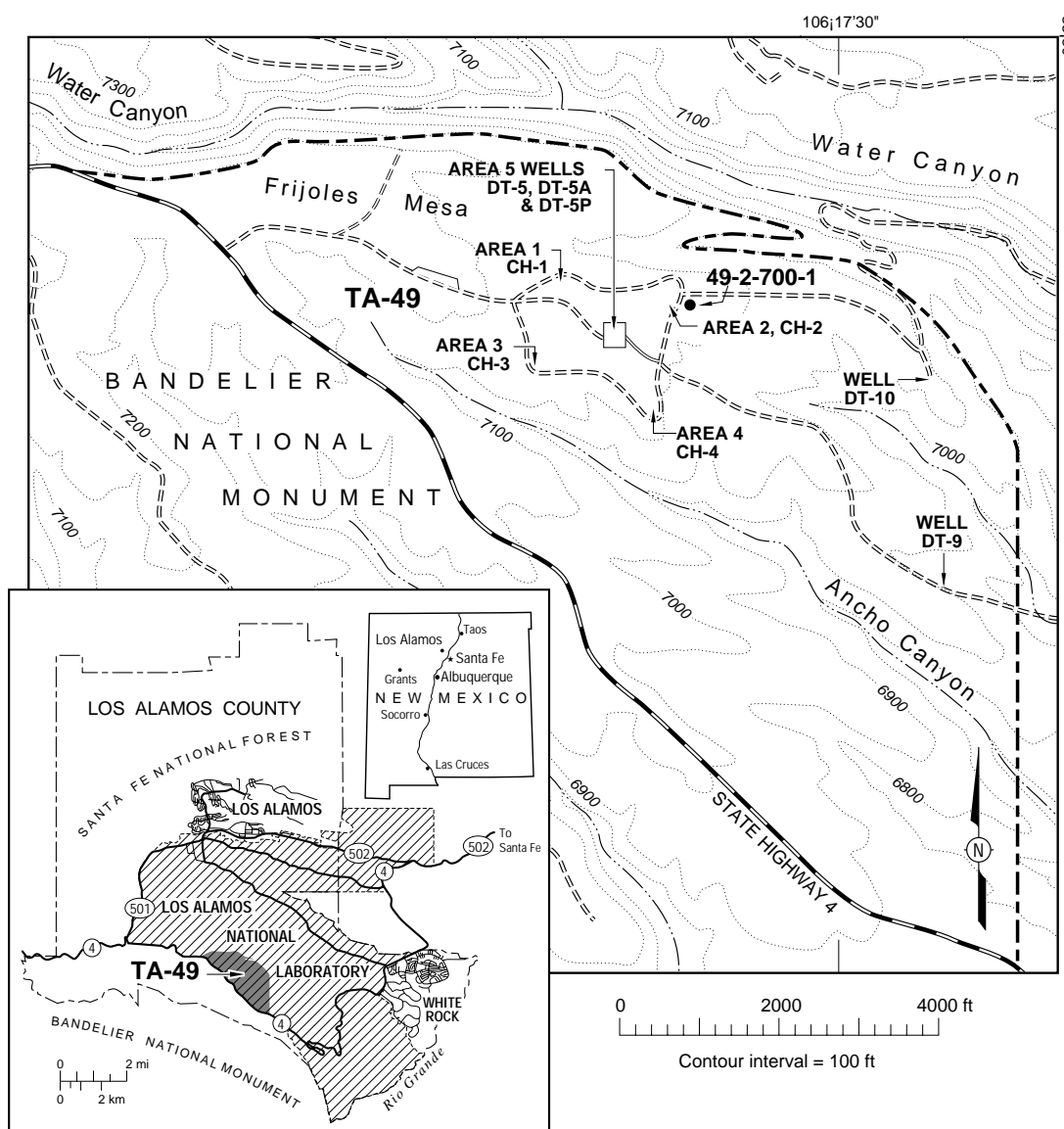


Figure 1. Map of the TA-49 area showing the location of borehole 49-2-700-1

This report provides geological data to develop and test hydrogeological conceptual models for the site and to evaluate potential transport pathways and processes. The data constrain numerical models for groundwater flow and contaminant transport, and they provide a geological framework for evaluating various types of remediation that could be applied at the site. Furthermore, this study delineates lithologic changes that may control the movement of moisture and contaminants.

The general stratigraphy of the Pajarito Plateau has been described by numerous authors (Griggs 1964; Smith and Bailey 1966; Broxton et al. 1995a; Broxton and Reneau 1995; and Goff 1995). Weir and Purtymun (1962) describe local geologic and hydrologic investigations conducted at TA-49 on Frijoles Mesa from 1959 to 1960. The purpose of the Weir and Purtymun investigation was to provide geologic information about the TA-49 site and to define the direction and rate of groundwater movement. Weir and Purtymun divided the Tshirege Member into six lithologic subunits as part of mapping and borehole studies. They determined the distribution of subsurface lithologic units by correlating lithologic and geophysical logs for borehole DT-5P, test wells DT-5, DT-5A, DT-9, and DT-10, and core holes CH-1, CH-2, CH-3, and CH-4 (Figure 1).

2.0 METHODS

A detailed graphic log was prepared for borehole 49-2-700-1 at the ER Project's Field Support Facility. This log can be obtained from the authors or through the Project's Record Processing Facility. A summary of the major lithologies in the borehole was prepared from the detailed graphic log and is presented as Figure 2.

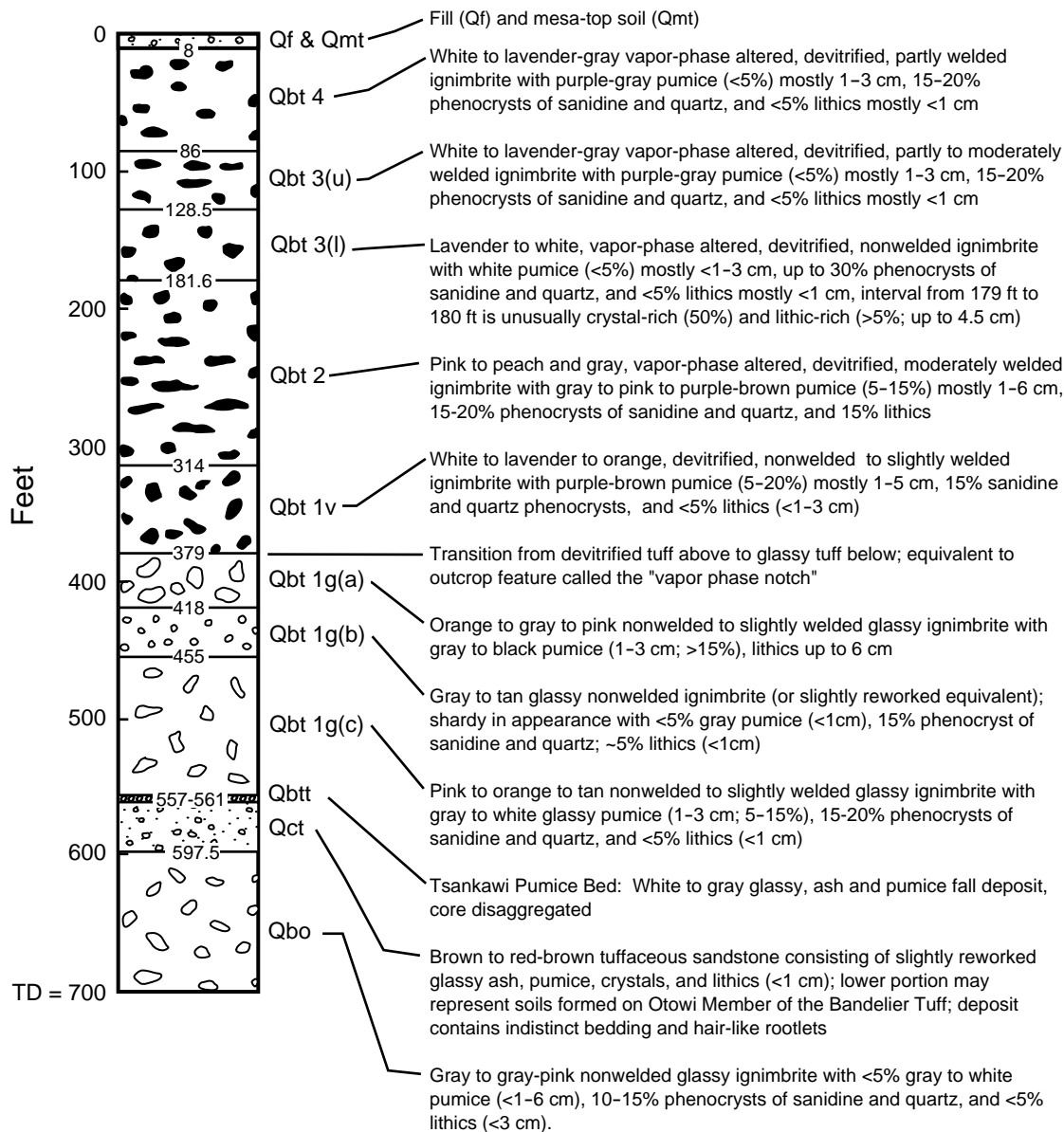
The graphic log includes descriptions of lithology, mineralogy, and abundances, sizes, and compositions of lithic fragments and pumice. Fractures and alteration patterns critical to assessing hydrologic flow paths are also described. Additional information recorded includes a summary of samples taken from the core and the state of core preservation.

Major and trace elements were analyzed in 64 samples using an automated Rigaku wavelength-dispersive X-ray fluorescence (XRF) spectrometer. Samples were prepared by crushing and homogenizing 15–20 g of the sample in a tungsten-carbide shatter box according to Yucca Mountain Project procedure LANL-EES-DP-130 (Geologic Sample Preparation). Sample splits were heated at 110°C for 24 hrs, and then 4-g splits were fused at 1100°C with 8 g of lithium metaborate/lithium tetraborate flux. Elemental concentrations were calculated by comparing X-ray intensities for the samples to those for 21 standards of known composition. A fundamental parameters program was used for matrix corrections (Criss 1980) in accordance with Yucca Mountain Project procedure LANL-EES-DP-111.

Splits of 39 XRF samples were sent to the US Geological Survey and analyzed for major and trace elements by instrumental neutron activation analysis (INAA). Baedeker and McKowen (1987) describe the INAA method and levels of precision and accuracy.

The mineralogy of the tuffs was determined by analyzing 63 samples using X-ray diffraction (XRD). Samples were first powdered in a tungsten-carbide shatter box and then mixed with an internal standard of 1 µm metallurgical grade Al₂O₃ (corundum) powder in a ratio of 80% sample to 20% internal standard by weight. The samples were then ground under acetone in an automatic Brinkmann-Retsch mill fitted with an agate mortar and pestle to produce an average particle size of less than 5 µm. This fine particle size is necessary to ensure adequate particle statistics and to minimize primary extinction (Klug and Alexander, 1974). Particle-size distributions have been verified in our laboratory for similar samples using a Horiba CAPA-500 centrifugal particle-size distribution analyzer calibrated with Duke Scientific

glass microsphere standards. X-ray diffraction data were collected on a Siemens D-500 theta-theta diffractometer using copper-K α radiation, incident- and diffracted-beam Soller slits and a Kevex solid-state (SiLi) detector. Data were typically collected from 2.0 to 50.0° 2 θ using a 0.02° step size and at least two seconds per step.



MAJOR STRATIGRAPHIC UNITS	
Qf	Fill
Qmt	Mesa top soil
Qct	Tephras and volcaniclastic sediments of the Cerro Toledo interval
Qbo	Otowi Member, Bandelier Tuff, undivided
Qbt 4	Tshirege Member, Bandelier Tuff Unit 4
Qbt 3	Unit 3: includes subunits Qbt 3(u) and Qbt 3(l)
Qbt 2	Unit 2
Qbt 1	Unit 1: includes subunits Qbt 1v and Qbt 1g as shown above; Qbt 1g is subdivided, in descending order, into Qbt 1g(a), Qbt 1g(b), and Qbt 1g(c).
Qbtt	Tsankawi Pumice Bed

Figure 2. Summary of major lithologies in borehole 49-2-700-1

Quantitative mineral analyses employed the internal standard or matrix-flushing method of Chung (1974a,b). Details of this method can be found in Bish and Chipera (1988; 1989). In addition, the following Yucca Mountain Project procedures were used for sample preparation and analysis of XRD samples: LANL-EES-DP-130 (Geologic Sample Preparation); LANL-EES-DP-56 (Brinkmann Automated Grinder Procedure); LANL-EES-DP-16 (Siemens X-Ray Diffraction Procedure); and LANL-EES-DP-116 (Quantitative X-Ray Diffraction Data Reduction Procedure). Yucca Mountain Project quality assurance requirements are comparable in rigor to those used by the LANL ER Project.

Moisture contents were determined gravimetrically on 128 samples collected at a nominal spacing of 5 ft. Samples were sealed in plastic bags as soon as possible after being collected from the borehole to prevent moisture loss. Samples from 0–468 ft were analyzed at an on-site mobile radiological laboratory. These samples were transferred to a clean container in a moisture analyzer where they were automatically weighed, dried at 200°C until they reached a constant mass, and weighed again. The remaining samples were analyzed by a fixed-base laboratory at CST-3. These samples were weighed, heated overnight in an oven at 100°C, and weighed again. The moisture data from the on-site mobile radiological laboratory and the fixed-base laboratory appear to be comparable based on the measured moisture contents and moisture trends for the entire borehole.

3.0 RESULTS AND DISCUSSION

3.1 Lithologies

Major lithologic units in the core are summarized in Figure 2, which uses the same symbol notation as the more detailed graphic log of Figure 1. The stratigraphic nomenclature follows the suggested usage of Broxton and Reneau (1995). Figure 3 compares the unit nomenclature used in this report with that used by Weir and Purtymun (1962), and it compares the stratigraphy of borehole 49-2-700-1 with nearby borehole DT-5P (see Figure 1 for location).

In descending order, the major units encountered in borehole 49-2-700-1 are as follows: (1) Qf (fill) and Qmt (mesa top soil); (2) units Qbt 4, Qbt 3, Qbt 2, Qbt 1v, Qbt 1g, and the Tsankawi Pumice Bed (Qbt) of the Tshirege Member of the Bandelier Tuff; (3) Qct, tephra and volcaniclastic sediments of the Cerro Toledo interval; and (4) Qbo, the Otowi Member of the Bandelier Tuff.

A few lithologic variations encountered in the core are open to interpretation, and ongoing study of core samples may require making minor modifications to the above unit designations. Of particular interest are variations in core designated as Qbt 1g of the Tshirege Member and Qct, the Cerro Toledo interval. In Figure 2 we divided Qbt 1g into three portions with distinctive features. Qbt 1g(a) is about 20 ft thick and similar to Qbt 1g at TA-21 (see Broxton et al. 1995a). It is nonwelded and grades in color from orange to gray; the pumices range in size mainly from 1–3 cm. Qbt 1g(b) is a distinctive facies consisting of about 37 ft of gray to tan, very fine-grained tephra and crystals; pumices are generally less than 1 cm. Qbt 1g(c) is similar to Qbt 1g(a) but with a slightly smaller average pumice size. It is likely that Qbt 1g(b) is a distinct facies that is not described elsewhere in the literature on the Bandelier Tuff. The origin of the fine-grained facies is not known at this time. Qct is mostly red-brown, fine-grained vitric tephra and crystals, which we currently interpret as a sequence of bedded tuffs, reworked tuffaceous sediments, and immature soils formed on a paleosurface incised into the top of the Otowi Member.

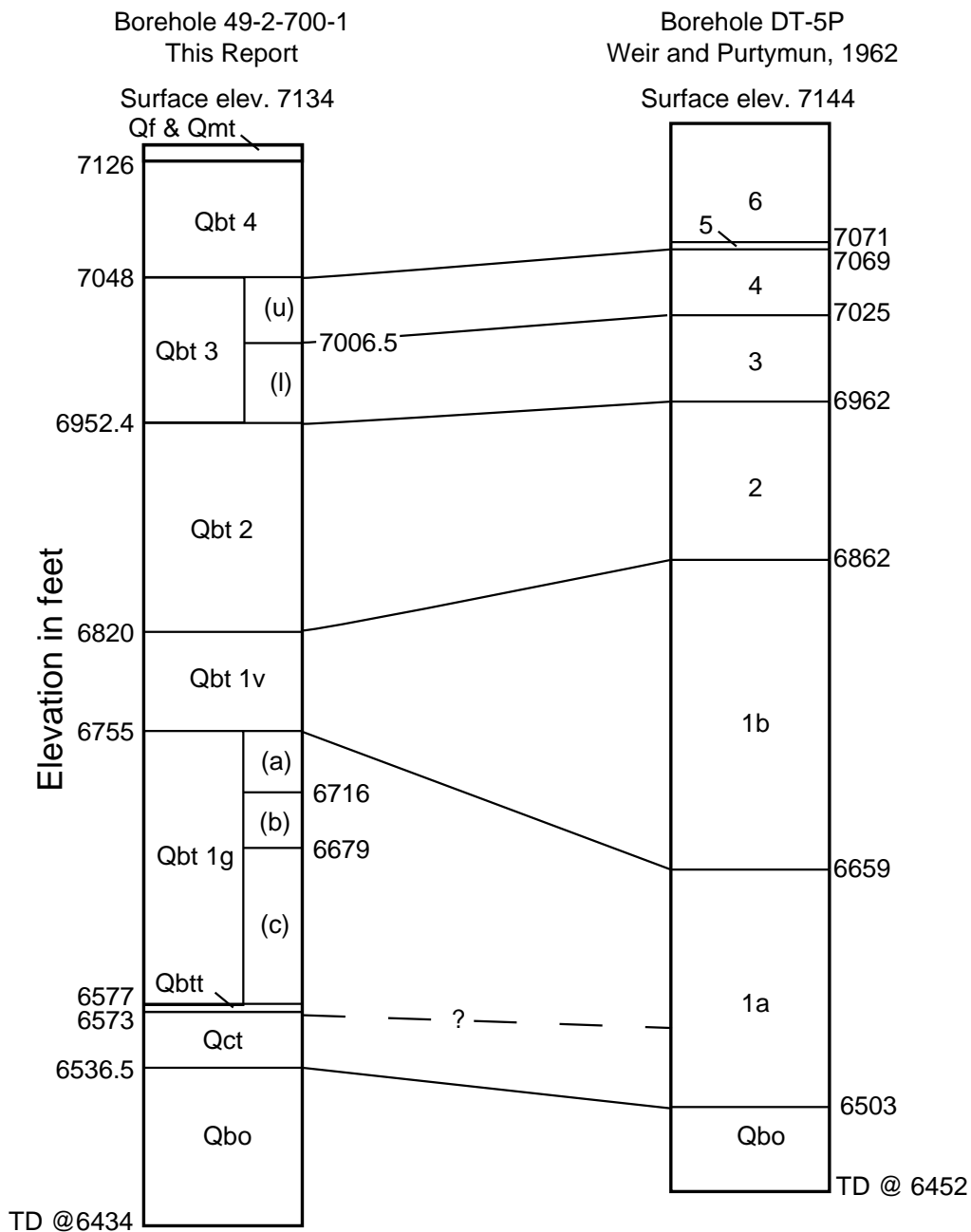


Figure 3. Correlation of stratigraphic units in borehole 49-2-700-1 with those described by Weir and Purtymun (1962) in nearby borehole DT-SP (unit correlations based on descriptions by Weir and Purtymun)

3.2 Moisture Distribution

Examination of moisture variations with depth in borehole 49-2-700-1 suggests some lithologic control. Gravimetric moisture contents are relatively high (11%) in fill material and soil (Qf and Qmf) near the surface, but they decrease abruptly to 1–4% in the upper tuff units of the Tshirege Member (Figure 4). Moisture contents are relatively constant in units Qbt 4, Qbt 3, Qbt 2, and the upper part of Qbt 1v, but they systematically increase in the central and lower part of Qbt 1v, culminating in a prominent moisture spike of 15% at the Qbt 1v/Qbt 1g contact (equivalent to the vapor phase notch in surface exposures). A similar moisture spike occurs at the Qbt 1v/Qbt 1g contact in borehole LADP-4 at TA-21 (Broxton et al. 1995b) and may represent a zone of preferential groundwater accumulation.

Below the moisture spike associated with the Qbt 1v/Qbt 1g contact, moisture contents generally range between 8–10% in subunits of Qbt 1g (Figure 4). Another prominent moisture spike begins in the lower part of Qbt 1g(c) and reaches a maximum of 16.5% in the Tsankawi Pumice Bed. This pattern of moisture distribution was also found in borehole LADP-4 (Broxton et al. 1995b). Below the Tsankawi Pumice Bed, moisture contents are somewhat erratic but typically range from 10–11%. The top of the main aquifer was not penetrated in borehole 49-2-700-1, but it is expected to be about 1163 ft deep based on nearby borehole DT-5A (Weir and Purtymun 1962).

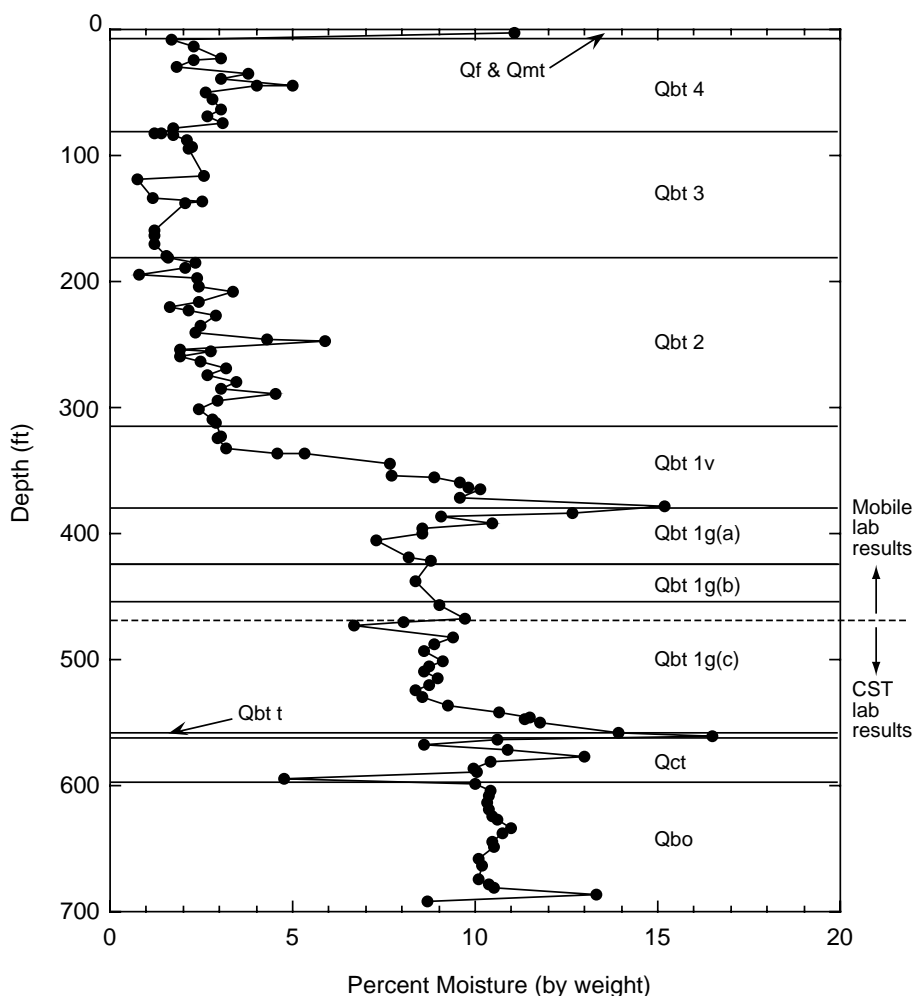


Figure 4. Comparison of moisture content with stratigraphic units of borehole 49-2-700-1

3.3 Fractures and Alteration

Only a few fractures were documented in the core, some of which lacked mineral coatings and may have been caused by drilling and sampling (e.g., fractures at 90 ft and 283 ft). A few irregular fractures with orange colored (limonitic?) staining are present in the first 35 ft of the core, and may influence hydrologic flow near the surface. At depths of >35 ft, only one region of the core, from 243 to 255 ft, showed four subvertical fractures with mineral coatings. The coatings consist primarily of smooth, orange-colored material 1–5 mm thick, which has tentatively been identified as a mixture of very fine-grained clays and Fe-oxides. Scanning electron microscopy indicates that the coatings consist primarily of Si, Al, and variable Fe, with lesser amounts of K and Ca, consistent with the tentatively identified mineralogy.

3.4 Chemistry

Bulk-rock chemical compositions for tuffs in borehole 49-2-700-1 by XRF are given in Appendix A, and INAA results are given in Appendix B. The Otowi Member and units Qbt 1g through Qbt 3 of the Tshirege Member are high-silica rhyolites (77% SiO₂, on a volatile-free basis), whereas Qbt 4 of the Tshirege Member is significantly less silicic (74% SiO₂). Major element abundances for these units show relatively little variability (except for Qbt 4), but both the Otowi and Tshirege Members are compositionally zoned with respect to their trace elements (Figure 5). Petrologic studies of the Bandelier Tuff have shown that these compositional zonations reflect the systematic withdrawal of magma from a chemically zoned magma chamber (Smith 1979). Compositional gaps occur at some unit boundaries, and they probably represent gaps in the depositional record of the Tshirege Member in this area. These gaps may represent the nondeposition of some tuffs at TA-49 because the runout of some ignimbrites from their source in the Valles caldera was limited to the western part of the Pajarito Plateau. Additionally, some ignimbrites from the Valles caldera may have flowed in directions other than towards the Pajarito Plateau.

The chemical data presented in Appendix A were combined with data from other sites across the Pajarito Plateau to establish whole-rock background elemental concentrations for the Bandelier Tuff. These background values were published as part of a separate report that summarizes a LANL-wide study to establish background levels for the ER Project (Ryti et al. 1998). It should be noted that the data presented in Appendix A are total elemental concentrations (as opposed to acid extractable concentrations), and their use for background concentrations is valid only if the analytical data being compared are also total elemental concentrations. The chemical data for the Bandelier Tuff show that its background chemistry varies as a function of stratigraphic position, particularly for trace elements (Figure 5).

The chemical data are also useful for establishing stratigraphic correlations of tuff units across the Pajarito Plateau. In drill holes, compositional gaps provide a means for recognizing unit boundaries (Figure 5). For example, Qbt 4 was not recognized during logging of the drill core for this borehole until the chemical data became available. Using chemical data in conjunction with the core logs increased the accuracy of our unit identifications. Correct placement of unit boundaries is critical for interpreting subsurface data and for selecting instrument locations in monitoring wells that target specific horizons.

3.5 Mineralogy

The pre-eruptive phenocryst assemblage of both the Tshirege and Otowi Members is dominated by alkali feldspar and quartz (generally from 10–25 vol %), with lesser amounts (<2 vol %) of Fe-rich pyroxene, Fe-Ti oxides, and fayalite, but they also contain other minerals at trace abundances (Warshaw and Smith 1988; Stimac 1996). Broxton et al. (1995a) provide more detailed information on the general modal petrography of the Bandelier Tuff and associated units.

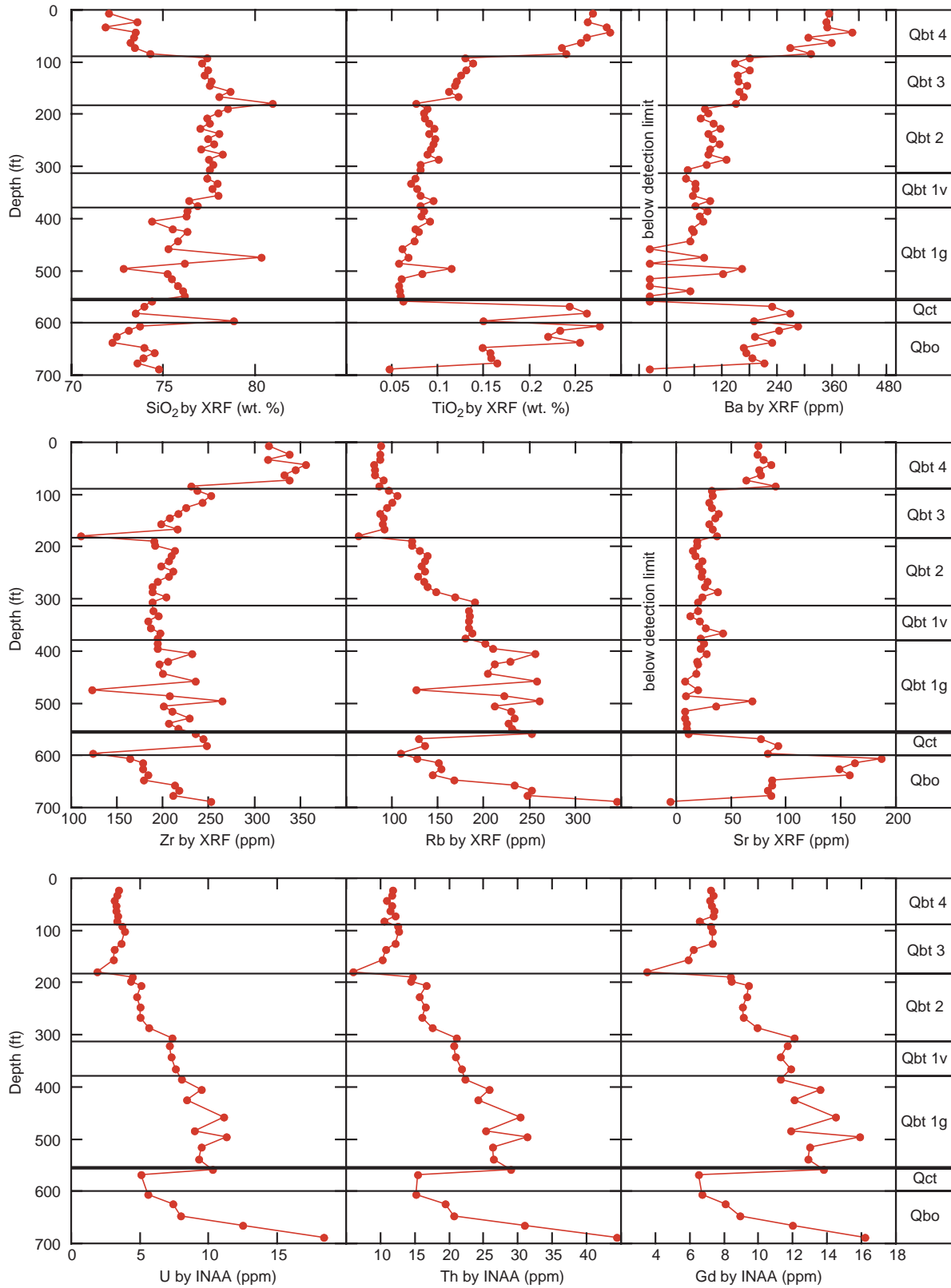


Figure 5. Comparison of chemical data with preliminary stratigraphic units of borehole 49-2-700-1

The bulk-tuff mineralogy of tuffs at TA-49 is relatively simple, consisting primarily of alkali feldspar + quartz ± cristobalite ± volcanic glass ± tridymite (Appendix C). These four minerals and the volcanic glass make up over 95% of nearly all tuff samples, although their relative proportions vary as a function of stratigraphic position (Figure 6). Minor constituents of the tuffs include smectite and hematite. Trace amounts of mica, hornblende, clinoptilolite, and kaolinite were also detected in a few of the samples.

Alkali feldspar and silica minerals have relatively poor ion-exchange properties and probably provide little in the way of natural mineralogic barriers to contaminant migration. On the other hand, the surfaces of these minerals have high affinities ($K_{ds} > 1000$ ml/g) for elements such as Am, Cm, Nb, REE, Sn, Th, Zr, and Pu (Allard et al. 1982; Beall and Allard 1981; Thomas 1987; Brandberg and Skagius 1991; Meijer 1992), and they may provide retardation by surface complexation.

Smectite, hematite, and Mn oxide are potentially important trace minerals because they are sorptive of certain radionuclides and could provide important natural barriers to their migration. Smectites are highly selective for cationic radionuclides (Grim 1968). Magnetite and its alteration products such as hematite have an affinity for uranium and actinide species through surface complexation (Hsi and Langmuir 1985; Ho and Miller 1986; Allard and Beall 1979; Beall and Allard 1981; and Allard et al. 1982). Mn oxides intergrown with clay minerals have an affinity for Pu, Ce, Ga, Nb, Pb, Y, Ca, Ti, and Zn (Duff et al. 2001). The clay-Mn oxide trace mineral assemblage has been identified in the Bandelier Tuff (both in the tuff matrix and as a fracture-filling material) and in overlying soils (Vaniman et al. 2002). Although the trace minerals described above occur in small quantities, they are disseminated throughout the stratigraphic sequence and may provide significant retardation potential over long groundwater flow paths.

Volcanic glass is the dominant mineralogic component of tuffs in Qbo, Qct, and Qbt 1g (Figure 6). The glass occurs as pumices, shaly tuff matrix, and fine ash. The presence of abundant glass and paucity of low-temperature alteration minerals such as smectites and zeolites indicate that the tuffs of Qbt 1g have had limited contact with groundwater since their deposition. Smectite is slightly more abundant (1 to 4% by weight) at the top of Qbo and in Qct (Figure 6), suggesting that a greater degree of low-temperature diagenetic alteration or soil clay development (possibly eolian) occurred in these units. The alteration in these tuffs and sediments may reflect incipient soil development resulting from a long period (~400,000 y) of surface exposure and weathering. The smectites abruptly disappear in Obtt, above Qct, suggesting that these clays formed prior to the deposition of the Tshirege Member.

Alkali feldspar, cristobalite, quartz, and tridymite are the main constituents of tuffs above the Qbt 1g/Qbt 1v contact (Figure 6). Alkali feldspar and cristobalite occur mainly in the tuff matrix as fine-grained (micron-size), high-temperature devitrification products that replaced the original volcanic glass as the tuff cooled. The tridymite and some alkali feldspar were deposited in open pore spaces by vapors released during outgassing of the tuff after emplacement. The stratigraphic association of tridymite and cristobalite with units Qbt 1v through Qbt 4 is similar to that reported for surface outcrops in Los Alamos Canyon (Broxton et al, 1995a). Tridymite is most abundant in Qbt 2 and Qbt 3, whereas cristobalite is most abundant in Qbt 1v and Qbt 4 (Fig. 6). Cristobalite and tridymite abundances vary inversely, suggesting that the occurrence of these minerals is controlled by a thermal or thermal-kinetic transition.

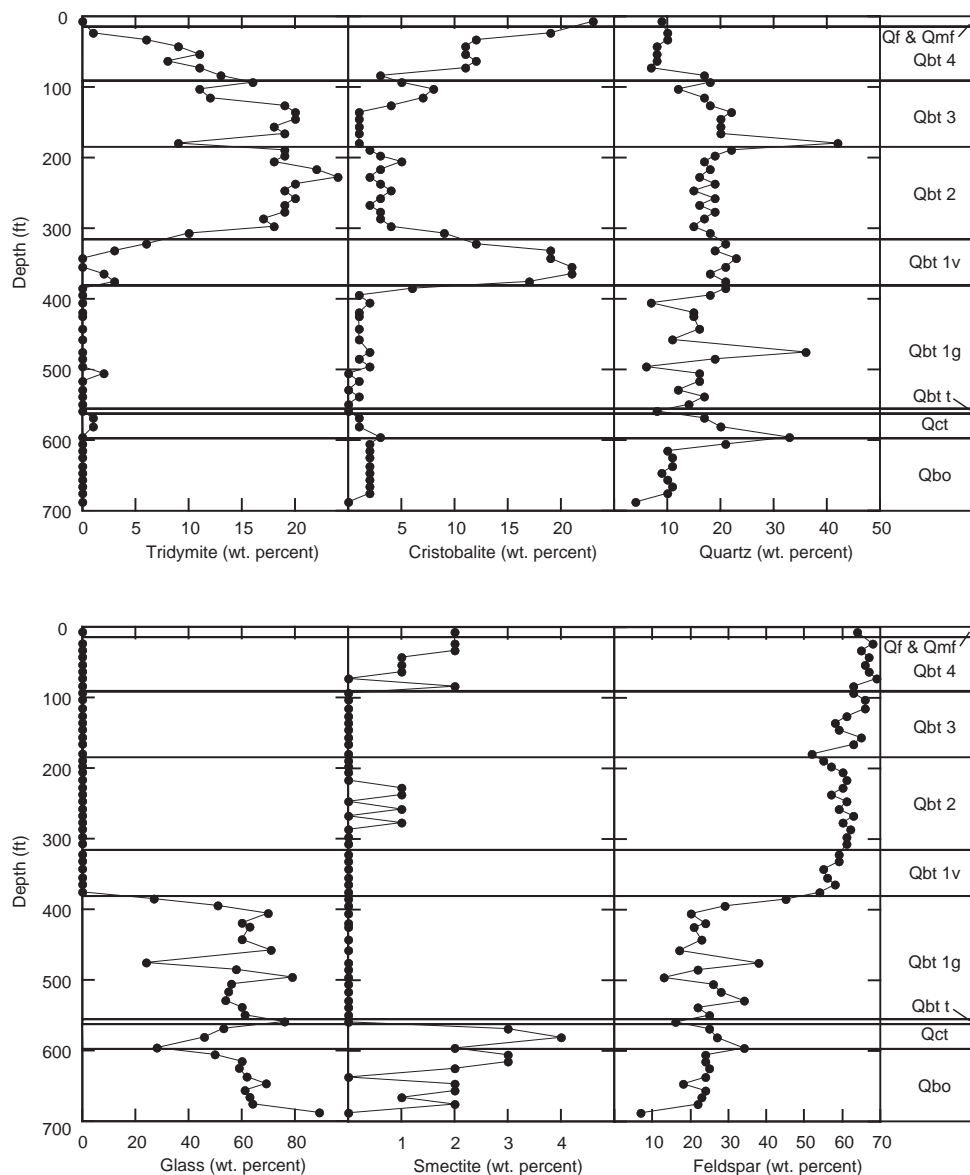


Figure 6. Comparison of mineralogical data with preliminary stratigraphic units of borehole 49-2-700-1

Tridymite is an indicator mineral for vapor-phase alteration, and its abundance in Qbt 2 and Qbt 3 suggests that post-emplacement vapor phase crystallization was greater in these tuffs relative to Qbt 1v and Qbt 4. The repetition of this alteration pattern over regional distances suggests that the eruptive hiatuses between units of the Tshirege Member were relatively brief, allowing the entire assemblage of units to devitrify together in a single stage. However, significant differences in degree of welding for adjacent units (e.g., Qbt 2 and Qbt 3[I]) indicate that eruptive hiatuses were of sufficient duration for distinct cooling breaks to develop.

Most of the alkali feldspar and quartz detected by XRD in the vitric tuffs of Qbo and Qbt 1g is coarse-grained (1–3 mm) phenocrysts that grew in the magma chamber prior to eruption (Broxton et al. 1995a). In Qbt 1v and higher units, the abrupt increase in alkali feldspar abundances over Qbt 1g and lower units reflects devitrification and vapor-phase crystallization (Figure 6). Quartz abundances are little affected by

the transition from vitric to devitrified tuffs in the Tshirege Member, suggesting that most or all of the quartz occurs as phenocrysts. The slight increase in quartz upsection through the Tshirege Member probably reflects the tendency for the unit to become more phenocryst-rich upsection (Broxton et al. 1995a). The abrupt decrease of quartz in Qbt 4 represents a fundamental change in the phenocryst assemblage of these uppermost tuffs, including a significant decrease in the quartz-to-alkali feldspar ratios (Figure 6).

Minor smectite and hematite occur in the devitrified tuffs of the Tshirege Member (Figure 6). Smectite is slightly more abundant at the top of Qbt 4 and may reflect post-Bandelier soil development. Although low in abundance, both minerals are widely disseminated through the tuffs and may inhibit the migration of radionuclides.

4.0 ACKNOWLEDGEMENTS

We thank Inez Triay, Cheryl Rofer, and John Hopkins of the ER Project for their programmatic support. The methods and terminology used to prepare the detailed petrologic log of corehole 49-2-700-1 were developed in consultation with J. Gardner and F. Caporuscio. Rebecca Brown-Gustin of ERM/Golder prepared an excellent on-site geologic log for this borehole, thus aiding us in our logging efforts. R. Warren, E. Springer, and D. Vaniman provided critical reviews of this report. R. Moore was the compositor, and M. Sachdeva was the editor.

5.0 REFERENCES

- B. Allard and G.W. Beall, "Sorption of Am on Geologic Media," *J. of Environ. Sci. and Health*, **A14** (6), 507–518 (1979).
- B. Allard, U. Olofsson, B. Torstenfelt, H. Kipasti, and H. Anderson, "Sorption of Actinides in Well-Defined Oxidation States on Geologic Media," in *Scientific Basis for Nuclear Waste Management V, Materials Research Society Symposia Proceedings*, L. Lutze, Ed. (Materials Research Society, Pittsburgh, Pennsylvania, 1982), pp. 775–786.
- P.A. Baedeker and D.M. McKowen, "Instrumental Neutron Activation Analysis of Geochemical Samples," in *Methods of Geochemical Analysis*, P.A. Baedeker, Ed., *US Geological Survey Bulletin* 1770 (1987).
- G.W. Beall and B. Allard, "Sorption of Actinides from Aqueous Solutions under Environmental Conditions," in *Proceedings of a Symposium on Adsorption from Aqueous Solutions* (American Chemical Society Meeting, Division of Colloid and Surface Chemistry, Houston, Texas, 1981), pp. 193–212.
- D.L. Bish and S.J. Chipera, "Problems and Solutions in Quantitative Analysis of Complex Mixtures by X-Ray Powder Diffraction," in *Advances in X-Ray Analysis* (Plenum Press, New York, 1988), Vol. 31, pp. 295–308.
- D.L. Bish and S.J. Chipera, "Revised Mineralogical Summary of Yucca Mountain, Nevada," Los Alamos National Laboratory report LA-11497-MS (1989).
- F. Brandberg and K. Skagius, "Porosity, Sorption, and Diffusivity Data Compiled for the SKB 91 Study," SKB Technical Report SKB-TR-91-16, Stockholm, Sweden (1991).

D.E. Broxton, G. Heiken, S.J. Chipera, and F.M. Byers, "Stratigraphy, Petrography, and Mineralogy of Bandelier Tuff and Cerro Toledo Deposits," in *Earth Science Investigations for Environmental Restoration—Los Alamos National Laboratory Technical Area 21*, D.E. Broxton and P.G. Eller, Eds., Los Alamos National Laboratory report LA-12934-MS (1995a [ER ID 50121]).

D.E. Broxton, P. Longmire, P.G. Eller, and D. Flores, "Preliminary Drilling Results for Boreholes LADP-3 and LADP-4," in *Earth Science Investigations for Environmental Restoration—Los Alamos National Laboratory Technical Area 21*, D.E. Broxton and P.G. Eller, Eds., Los Alamos National Laboratory report LA-12934-MS, pp. 93–109 (1995b [ER ID 50119]).

D.E. Broxton and S.L. Reneau, "Stratigraphic Nomenclature of the Bandelier Tuff for the Environmental Restoration Project at Los Alamos National Laboratory," Los Alamos National Laboratory report LA-13010-MS (1995 [ER ID 49726]).

F.H. Chung, "Quantitative Interpretation of X-Ray Diffraction Patterns of Mixtures: I. Matrix-Flushing Method for Quantitative Multicomponent Analysis," *J. Appl. Crystallogr.* **7**, 519–525 (1974a).

F.H. Chung, "Quantitative Interpretation of X-Ray Diffraction Patterns of Mixtures: II. Adiabatic Principle of X-Ray Diffraction Analysis of Mixtures," *J. Appl. Crystallogr.* **7**, 526–531 (1974b).

J. Criss, "Fundamental Parameters Calculations on a Laboratory Microcomputer," *Adv. X-Ray Anal.* **23**, 93–97 (1980).

M.C. Duff, D.B. Hunter, I.R. Triay, P.M. Bertsch, J. Kitten, and D.T. Vaniman, "Comparison of Two Micro-Analytical Methods for Detecting the Spatial Distribution of Sorbed Pu on Geologic Materials," *J. Contam. Hydrol.* **47**, pp. 211–218 (2001 [ER ID 73281]).

F. Goff, "Geologic Map of Technical Area 21, Los Alamos National Laboratory, New Mexico," in *Earth Science Investigations for Environmental Restoration—Los Alamos National Laboratory Technical Area 2*, D.E. Broxton and P.G. Eller, Eds., Los Alamos National Laboratory report LA-12934-MS, pp. 7–18 (1995 [ER ID 49682]).

R.E. Grim, *Clay Mineralogy*, 2nd ed. (McGraw-Hill Book Company, New York, 1968).

R.L. Griggs, "Geology and Ground-Water Resources of the Los Alamos Area, New Mexico," US Geological Survey Water-Supply Paper 1753 (1964 [ER ID 65649]).

C.H. Ho and N.H. Miller, "Adsorption of Uranyl Species from Bicarbonate Solution onto Hematite Particles," *J. Colloid Interface Sci.* **110**, 165–171 (1986).

C-K. Hsi and D. Langmuir, "Adsorption of Uranyl onto Ferric Oxyhydroxides: Application of the Surface Complexation Site-Binding Model," *Geochim. Cosmochim. Acta* **49**, 1931–1941 (1985).

H. P. Klug and L.E. Alexander, *X-Ray Diffraction Procedures for Polycrystalline and Amorphous Materials* (John Wiley & Sons, Inc, New York, 1974).

A. Meijer, "Experiments and Integration of Relevant Sorption Models," in *DOE/Site Characterization Project Radionuclide Adsorption Workshop, Los Alamos National Laboratory*, Los Alamos National Laboratory Conference report LA-12325-C (1992).

R.T. Rytí, P. Longmire, D.E. Broxton, S.L. Reneau, and E.V. McDonald, "Inorganic and Radionuclide Background Data for Soils, Canyon Sediments, and Bandelier Tuff at Los Alamos National Laboratory," Los Alamos National Laboratory document LA-UR-98-4847 (1998 [ER ID 59730]).

R.L. Smith and R.A. Bailey, "The Bandelier Tuff: A Study of Ash-Flow Eruption Cycles and Zoned Magma Chambers, *Bull. Volcanol.* **29**, 83–104 (1966 [ER ID 21584]).

R.L. Smith, "Ash-Flow Magmatism," *Geol. Soc. Am. Spec.*, Pap. 180, 5–28 (1979).

J. Stimac, "Hornblende-Dactite Pumice in the Tshirege Member of the Bandelier Tuff: Implications for Magma Chamber and Eruptive Processes," in *The Jemez Mountain Region*, F. Goff et al. Eds. (New Mexico Geological Society Guidebook, 1996), pp. 269–274.

K.W. Thomas, "Summary of Sorption Measurements Performed with Yucca Mountain, Nevada, Tuff Samples and Water from Well J-13," Los Alamos National Laboratory report LA-10969-MS (1987).

D.T. Vaniman, S.J. Chipera, L.D. Bish, M.C. Duff, and D.B. Hunter, "Crystal Chemistry of Clay-Mn Oxide Associations in Soils, Fractures, and Matrix of the Bandelier Tuff, Pajarito Mesa, New Mexico," *Geochim. Cosmochim. Acta*, **66**, 1349–1374 (2002 [ER ID 73280]).

C.M. Warshaw and R.L. Smith, "Pyroxenes and Fayalites in the Bandelier Tuff, New Mexico: Temperatures and Comparison with Other Rhyolites," *Am. Mineral.*, **73**, 1025–1037 (1988).

J.E. Weir and W.D. Purtymun, "Geology and Hydrology of Technical Area 49, Frijoles Mesa, Los Alamos County, New Mexico," US Geological Survey Administration Release report, Albuquerque, NM (1962).

Appendix A

Bulk-Rock Chemical Compositions for Borehole 49-2-700-1

APPENDIX A. BULK-ROCK CHEMICAL COMPOSITIONS FOR BOREHOLE 49-2-700-1¹

Sample Number	49-2-7.1	49-2-23.1	49-2-33.0	49-2-43.0	49-2-53.0	49-2-63.0	49-2-73.0	49-2-83.7	49-2-93.0	49-2-103.0
Depth (ft.)	7.1	23.1	33.0	43.0	53.0	63.0	73.0	83.7	93.0	103.0
Strat. Unit	Qf-Qmt	Qbt 4	Qbt 3	Qbt 3						
XRF file	BRO269	BRO271	BRO271							
Fusion Number	5064	5065	5066	5067	5068	5069	5070	5071	5072	5073
Major Elements (wt. %)										
SiO ₂	72.0 ± 0.9	73.6 ± 0.9	71.8 ± 0.9	73.5 ± 0.9	73.4 ± 0.9	73.2 ± 0.9	73.5 ± 0.9	74.3 ± 1.0	77.4 ± 1.0	77.1 ± 1.0
TiO ₂	0.27 ± 0.01	0.26 ± 0.01	0.28 ± 0.01	0.29 ± 0.01	0.26 ± 0.01	0.26 ± 0.01	0.24 ± 0.01	0.24 ± 0.01	0.13 ± 0.01	0.14 ± 0.01
Al ₂ O ₃	13.7 ± 0.2	13.2 ± 0.2	13.9 ± 0.2	13.4 ± 0.2	13.2 ± 0.2	13.1 ± 0.2	13.1 ± 0.2	12.6 ± 0.2	12.2 ± 0.2	12.1 ± 0.2
Fe ₂ O ₃ T	2.56 ± 0.06	2.44 ± 0.06	2.66 ± 0.06	2.39 ± 0.06	2.26 ± 0.06	2.21 ± 0.06	2.12 ± 0.06	2.26 ± 0.06	1.54 ± 0.06	1.62 ± 0.06
MnO	0.06 ± 0.01	0.07 ± 0.01	0.07 ± 0.01	0.08 ± 0.01	0.07 ± 0.01	0.07 ± 0.01	0.07 ± 0.01	0.08 ± 0.01	0.05 ± 0.01	0.06 ± 0.01
MgO	0.39 ± 0.07	0.24 ± 0.07	0.36 ± 0.07	0.32 ± 0.07	0.25 ± 0.07	0.24 ± 0.07	0.18 ± 0.07	0.37 ± 0.07	-0.08	0.08 ± 0.08
CaO	0.80 ± 0.11	0.85 ± 0.11	0.92 ± 0.11	0.97 ± 0.11	0.80 ± 0.11	0.82 ± 0.11	0.65 ± 0.11	0.91 ± 0.11	0.37 ± 0.11	0.39 ± 0.11
Na ₂ O	4.00 ± 0.09	4.28 ± 0.09	4.20 ± 0.09	4.53 ± 0.09	4.43 ± 0.09	4.44 ± 0.09	4.48 ± 0.09	4.17 ± 0.09	4.16 ± 0.09	4.20 ± 0.09
K ₂ O	4.33 ± 0.05	4.56 ± 0.05	4.29 ± 0.05	4.54 ± 0.05	4.57 ± 0.05	4.55 ± 0.05	4.68 ± 0.05	4.22 ± 0.05	4.50 ± 0.05	4.57 ± 0.05
P ₂ O ₅	0.05 ± 0.01	0.05 ± 0.01	0.06 ± 0.01	0.06 ± 0.01	0.05 ± 0.01	0.05 ± 0.01	0.04 ± 0.01	0.05 ± 0.01	-0.01	-0.01
LOI %	1.39	0.38	1.08	0.21	0.12	0.18	0.17	0.16	0.08	0.13
Total	99.6	99.9	99.6	100.3	99.4	99.1	99.2	99.3	100.4	100.4
Trace Elements (ppm)										
V	20 ± 8	19 ± 8	8 ± 8	11 ± 8	13 ± 8	-8	8 ± 8	17 ± 8	-7	-7
Cr	12 ± 8	-8	10 ± 8	-8	-8	-8	-8	14 ± 8	-8	-8
Ni	9 ± 6	-6	-6	-6	-6	-6	-6	8 ± 6	-6	-6
Zn	64 ± 9	61 ± 9	62 ± 9	55 ± 8	62 ± 9	50 ± 8	60 ± 9	101 ± 11	50 ± 8	51 ± 8
Rb	88 ± 6	86 ± 6	87 ± 6	80 ± 6	81 ± 6	81 ± 6	90 ± 6	86 ± 6	96 ± 6	105 ± 6
Sr	75 ± 5	74 ± 5	80 ± 5	86 ± 5	75 ± 5	77 ± 5	64 ± 5	90 ± 5	32 ± 5	33 ± 5
Y	30 ± 4	34 ± 4	32 ± 4	33 ± 4	39 ± 4	34 ± 4	36 ± 5	32 ± 4	35 ± 4	36 ± 5
Zr	316 ± 15	338 ± 16	315 ± 15	356 ± 16	345 ± 16	332 ± 16	338 ± 16	231 ± 13	237 ± 13	253 ± 14
Nb	44 ± 5	42 ± 5	43 ± 5	38 ± 5	40 ± 5	39 ± 6	45 ± 6	40 ± 5	44 ± 6	51 ± 6
Ba	354 ± 27	349 ± 27	350 ± 27	404 ± 28	308 ± 27	359 ± 27	269 ± 26	314 ± 27	181 ± 25	149 ± 25

¹ Elemental abundances determined by X-ray fluorescence; uncertainties are two standard deviation estimates of analytical precision. Concentrations preceded by a negative sign are below detection limit. Errors cited are analyzed ($\pm 2\sigma$); negative values indicate detection limits, with no detection.

Sample Number	49-2-115.0	49-2-126.0	49-2-136.7	49-2-145.0	49-2-156.0	49-2-166.9	49-2-179.0	49-2-189.1	49-2-197.6	49-2-206.8
Depth (ft.)	115.0	126.0	136.7	145.0	156.0	166.9	179.0	189.1	197.6	206.8
Strat. Unit	Qbt 3	Qbt 2	Qbt 2	Qbt 2						
XRF file	BRO271	BRO271	BRO270	BRO276						
Fusion Number	5074	5075	5076	5077	5078	5079	5080	5081	5082	5212

<u>Major Elements (wt. %)</u>	
SiO ₂	77.4 ± 1.0
TiO ₂	0.13 ± 0.01
Al ₂ O ₃	12.0 ± 0.2
Fe ₂ O ₃ T	1.54 ± 0.06
MnO	0.05 ± 0.01
MgO	-0.08
CaO	0.36 ± 0.11
Na ₂ O	4.16 ± 0.09
K ₂ O	4.50 ± 0.05
P ₂ O ₅	-0.01
LOI %	0.11
Total	100.3

<u>Trace Elements (ppm)</u>	
V	-7
Cr	-8
Ni	-6
Zn	56 ± 9
Rb	100 ± 6
Sr	30 ± 5
Y	41 ± 5
Zr	243 ± 14
Nb	44 ± 6
Ba	181 ± 25

Sample Number	49-2-217.0	49-2-227.3	49-2-237.0	49-2-247.0	49-2-257.0	49-2-267.0	49-2-277.3	49-2-287.0	49-2-297.0	49-2-307.0
Depth (ft.)	217.0	227.3	237.0	247.0	257.0	267.0	277.3	287.0	297.0	307.0
Strat. Unit	Qbt 2									
XRF file	BRO270	BRO271	BRO271	BRO271	BRO271	BRO272	BRO272	BRO272	BRO272	BRO272
Fusion Number	5083	5084	5085	5086	5087	5088	5089	5090	5091	5092

Major Elements (wt. %)

SiO ₂	77.5 ± 1.0	77.0 ± 1.0	78.0 ± 1.0	77.4 ± 1.0	77.8 ± 1.0	77.0 ± 1.0	78.2 ± 1.0	77.5 ± 1.0	77.7 ± 1.0	77.5 ± 1.0
TiO ₂	0.09 ± 0.02	0.10 ± 0.02	0.09 ± 0.02	0.10 ± 0.02	0.09 ± 0.02	0.09 ± 0.02	0.09 ± 0.02	0.10 ± 0.02	0.08 ± 0.02	0.08 ± 0.02
Al ₂ O ₃	11.5 ± 0.3	11.5 ± 0.3	11.3 ± 0.3	11.8 ± 0.3	11.5 ± 0.3	11.5 ± 0.3	11.5 ± 0.3	11.6 ± 0.3	11.6 ± 0.3	11.4 ± 0.3
Fe ₂ O ₃ T	1.41 ± 0.06	1.49 ± 0.06	1.43 ± 0.06	1.50 ± 0.06	1.46 ± 0.06	1.43 ± 0.06	1.47 ± 0.06	1.59 ± 0.06	1.48 ± 0.06	1.49 ± 0.06
MnO	0.06 ± 0.01	0.06 ± 0.01	0.06 ± 0.01	0.06 ± 0.01	0.06 ± 0.01	0.06 ± 0.01	0.06 ± 0.01	0.07 ± 0.01	0.06 ± 0.01	0.07 ± 0.01
MgO	-0.08	-0.08	-0.08	-0.08	-0.08	-0.08	-0.08	0.09 ± 0.08	-0.08	-0.08
CaO	0.29 ± 0.11	0.31 ± 0.11	0.29 ± 0.11	0.28 ± 0.11	0.25 ± 0.11	0.28 ± 0.11	0.29 ± 0.11	0.35 ± 0.11	0.29 ± 0.11	0.28 ± 0.11
Na ₂ O	4.05 ± 0.09	4.05 ± 0.09	3.94 ± 0.08	4.08 ± 0.09	4.06 ± 0.09	4.04 ± 0.09	3.96 ± 0.09	4.08 ± 0.09	4.17 ± 0.09	4.03 ± 0.09
K ₂ O	4.38 ± 0.05	4.35 ± 0.05	4.30 ± 0.05	4.39 ± 0.05	4.30 ± 0.05	4.21 ± 0.05	4.19 ± 0.05	4.20 ± 0.05	4.30 ± 0.05	4.29 ± 0.05
P ₂ O ₅	-0.01	-0.01	-0.01	-0.01	-0.01	-0.01	-0.01	-0.01	-0.01	-0.01
LOI %	0.11	0.15	0.21	0.24	0.15	0.16	0.29	0.28	0.21	0.18
Total	99.4	99.1	99.7	99.9	99.6	98.8	100.1	99.8	99.9	99.3

Trace Elements (ppm)

V	-7	-7	8 ± 7	10 ± 7	9 ± 7	-7	-7	-7	-7	-7
Cr	-8	-8	-8	-8	-8	-8	-8	-8	-8	-8
Ni	-6	7 ± 6	-6	-6	-6	-6	-6	11 ± 6	-6	-6
Zn	62 ± 9	63 ± 9	37 ± 8	62 ± 9	57 ± 9	59 ± 9	50 ± 8	81 ± 10	83 ± 10	65 ± 9
Rb	138 ± 6	135 ± 6	131 ± 6	135 ± 6	128 ± 6	134 ± 6	139 ± 6	148 ± 6	168 ± 7	190 ± 7
Sr	17 ± 5	23 ± 5	21 ± 5	24 ± 5	23 ± 5	28 ± 5	26 ± 5	38 ± 5	24 ± 5	20 ± 5
Y	50 ± 5	48 ± 5	49 ± 5	48 ± 5	50 ± 5	51 ± 5	58 ± 6	56 ± 6	71 ± 6	68 ± 6
Zr	209 ± 13	206 ± 13	197 ± 13	211 ± 13	207 ± 13	194 ± 13	189 ± 12	188 ± 12	203 ± 13	189 ± 12
Nb	65 ± 6	59 ± 6	59 ± 6	64 ± 6	60 ± 6	58 ± 6	60 ± 6	65 ± 6	76 ± 7	81 ± 7
Ba	101 ± 26	117 ± 25	90 ± 26	99 ± 26	115 ± 25	94 ± 25	89 ± 26	130 ± 25	87 ± 26	46 ± 27

Sample Number	49-2-322.7	49-2-332.2	49-2-342.0	49-2-355.2	49-2-365.2	49-2-375.0	49-2-385.0	49-2-395.0	49-2-405.4	49-2-419.4
Depth (ft.)	322.7	332.2	342.0	355.2	365.2	375.0	385.0	395.0	405.4	419.4
Strat. Unit	Qbt 1v	Qbt 1g	Qbt 1g	Qbt 1g	Qbt 1g					
XRF file	BRO272	BRO272	BRO272	BRO273	BRO273	BRO272	BRO272	BRO273	BRO273	BRO273
Fusion Number	5093	5094	5095	5096	5097	5098	5099	5100	5101	5102

Major Elements (wt. %)

SiO ₂	77.4 ± 1.0	78.0 ± 1.0	77.7 ± 1.0	78.0 ± 1.0	76.4 ± 1.0	76.9 ± 1.0	76.3 ± 1.0	76.3 ± 1.0	74.4 ± 1.0	75.5 ± 1.0
TiO ₂	0.08 ± 0.02	0.07 ± 0.02	0.08 ± 0.02	0.08 ± 0.02	0.09 ± 0.02	0.08 ± 0.02	0.08 ± 0.02	0.08 ± 0.02	0.09 ± 0.02	0.08 ± 0.02
Al ₂ O ₃	11.3 ± 0.3	11.3 ± 0.3	11.3 ± 0.3	11.1 ± 0.3	11.7 ± 0.3	11.5 ± 0.3	11.5 ± 0.3	11.3 ± 0.3	11.8 ± 0.3	11.5 ± 0.3
Fe ₂ O ₃ T	1.39 ± 0.06	1.39 ± 0.06	1.40 ± 0.06	1.40 ± 0.06	1.53 ± 0.06	1.40 ± 0.06	1.48 ± 0.06	1.14 ± 0.06	1.73 ± 0.06	1.51 ± 0.06
MnO	0.06 ± 0.01	0.06 ± 0.01	0.06 ± 0.01	0.06 ± 0.01	0.07 ± 0.01	0.06 ± 0.01	0.07 ± 0.01	0.06 ± 0.01	0.07 ± 0.01	0.07 ± 0.01
MgO	-0.08	-0.08	-0.08	-0.08	0.08 ± 0.08	-0.08	-0.08	-0.08	0.09 ± 0.08	-0.08
CaO	0.25 ± 0.11	0.22 ± 0.11	0.29 ± 0.11	0.27 ± 0.11	0.34 ± 0.11	0.32 ± 0.11	0.33 ± 0.11	0.32 ± 0.11	0.31 ± 0.11	0.31 ± 0.11
Na ₂ O	4.10 ± 0.09	4.13 ± 0.09	3.99 ± 0.09	3.97 ± 0.09	4.18 ± 0.09	3.92 ± 0.08	3.86 ± 0.08	3.59 ± 0.08	3.68 ± 0.08	3.78 ± 0.08
K ₂ O	4.23 ± 0.05	4.29 ± 0.05	4.16 ± 0.05	4.14 ± 0.05	4.25 ± 0.05	4.21 ± 0.05	4.35 ± 0.05	4.61 ± 0.05	4.81 ± 0.05	4.35 ± 0.05
P ₂ O ₅	-0.01	-0.01	-0.01	-0.01	0.02 ± 0.01	-0.01	-0.01	-0.01	-0.01	-0.01
LOI %	0.26	0.27	0.47	0.39	0.47	0.57	0.90	1.44	1.92	1.98
Total	99.0	99.7	99.3	99.4	99.1	98.9	98.8	98.8	98.9	99.0

Trace Elements (ppm)

V	7 ± 7	-7	-7	-7	-7	-7	-7	-7	-7	-7
Cr	-8	-8	-8	-8	-8	-8	-8	-8	-8	-8
Ni	-6	-6	-6	-6	-6	-6	-6	-6	-6	-6
Zn	64 ± 9	67 ± 9	64 ± 9	109 ± 12	217 ± 20	71 ± 10	97 ± 11	32 ± 7	70 ± 9	74 ± 10
Rb	184 ± 7	184 ± 7	183 ± 7	183 ± 7	188 ± 7	180 ± 7	201 ± 7	210 ± 7	256 ± 7	229 ± 7
Sr	20 ± 5	12 ± 5	21 ± 5	27 ± 5	42 ± 5	22 ± 5	25 ± 5	22 ± 5	27 ± 5	19 ± 5
Y	68 ± 6	72 ± 6	68 ± 6	72 ± 6	72 ± 6	69 ± 6	73 ± 6	74 ± 6	83 ± 8	83 ± 7
Zr	189 ± 12	195 ± 13	183 ± 12	186 ± 12	197 ± 13	194 ± 13	194 ± 13	194 ± 12	232 ± 13	205 ± 13
Nb	87 ± 7	83 ± 7	83 ± 7	80 ± 7	92 ± 7	88 ± 7	87 ± 7	90 ± 7	102 ± 9	104 ± 9
Ba	41 ± 27	62 ± 26	62 ± 27	57 ± 26	93 ± 26	62 ± 27	89 ± 26	71 ± 26	79 ± 26	54 ± 26

Sample Number	49-2-425.8	49-2-443.2	49-2-458.0	49-2-475.0	49-2-485.7	49-2-496.5	49-2-506.4	49-2-516.0	49-2-529.0	49-2-539.0
Depth (ft.)	425.8	443.2	458.0	475.0	485.7	496.5	506.4	516.0	529.0	539.0
Strat. Unit	Qbt 1g									
XRF file	BRO273	BRO274	BRO275							
Fusion Number	5103	5104	5105	5106	5107	5108	5109	5110	5111	5112
<u>Major Elements (wt. %)</u>										
SiO ₂	76.3 ± 1.0	75.8 ± 1.0	75.2 ± 1.0	80.4 ± 1.0	76.1 ± 1.0	72.8 ± 0.9	75.2 ± 1.0	75.5 ± 1.0	75.8 ± 1.0	76.1 ± 1.0
TiO ₂	0.08 ± 0.02	0.07 ± 0.02	0.06 ± 0.02	0.07 ± 0.02	0.06 ± 0.02	0.12 ± 0.01	0.08 ± 0.02	0.06 ± 0.02	0.06 ± 0.02	0.06 ± 0.02
Al ₂ O ₃	11.4 ± 0.3	11.3 ± 0.3	11.6 ± 0.3	9.7 ± 0.3	11.2 ± 0.3	12.3 ± 0.2	11.5 ± 0.3	11.3 ± 0.3	11.4 ± 0.3	11.1 ± 0.3
Fe ₂ O ₃ T	1.49 ± 0.06	1.43 ± 0.06	1.56 ± 0.06	1.26 ± 0.06	1.09 ± 0.06	1.96 ± 0.06	1.56 ± 0.06	1.40 ± 0.06	1.45 ± 0.06	1.43 ± 0.06
MnO	0.07 ± 0.01	0.07 ± 0.01	0.08 ± 0.01	0.06 ± 0.01	0.07 ± 0.01	0.09 ± 0.01	0.07 ± 0.01	0.07 ± 0.01	0.08 ± 0.01	0.08 ± 0.01
MgO	-0.08	-0.08	-0.08	0.08 ± 0.08	-0.08	0.24 ± 0.07	0.13 ± 0.07	-0.08	-0.08	-0.08
CaO	0.32 ± 0.11	0.31 ± 0.11	0.26 ± 0.11	0.32 ± 0.11	0.25 ± 0.11	0.67 ± 0.11	0.47 ± 0.11	0.26 ± 0.11	0.26 ± 0.11	0.27 ± 0.11
Na ₂ O	3.82 ± 0.08	3.71 ± 0.08	3.88 ± 0.08	3.29 ± 0.08	3.79 ± 0.08	3.99 ± 0.09	3.96 ± 0.09	3.90 ± 0.08	4.01 ± 0.09	3.88 ± 0.08
K ₂ O	4.19 ± 0.05	4.17 ± 0.05	4.36 ± 0.05	3.53 ± 0.05	4.16 ± 0.05	4.06 ± 0.05	4.10 ± 0.05	4.17 ± 0.05	4.26 ± 0.05	4.14 ± 0.05
P ₂ O ₅	-0.01	-0.01	-0.01	-0.01	-0.01	0.02 ± 0.01	-0.01	-0.01	-0.01	-0.01
LOI %	1.95	1.89	2.10	0.93	2.03	2.34	1.60	1.94	1.92	1.86
Total	99.6	98.7	99.1	99.6	98.7	98.6	98.7	98.6	99.2	98.8
<u>Trace Elements (ppm)</u>										
V	-7	-7	-7	-7	-7	-7	-7	-7	-7	9 ± 7
Cr	-8	-8	-8	-8	-8	-8	-8	-8	-8	-8
Ni	-6	7 ± 6	-6	-6	-6	9 ± 6	7 ± 6	-6	-6	-6
Zn	88 ± 11	92 ± 11	109 ± 12	60 ± 9	25 ± 7	264 ± 24	89 ± 11	74 ± 10	92 ± 11	107 ± 12
Rb	212 ± 7	204 ± 7	257 ± 7	126 ± 6	222 ± 7	261 ± 7	211 ± 7	230 ± 7	234 ± 7	227 ± 7
Sr	20 ± 5	18 ± 5	8 ± 5	20 ± 5	9 ± 5	69 ± 5	36 ± 5	8 ± 5	8 ± 5	10 ± 5
Y	75 ± 7	81 ± 7	102 ± 9	42 ± 5	82 ± 8	113 ± 10	78 ± 7	84 ± 8	94 ± 8	93 ± 8
Zr	196 ± 13	200 ± 13	235 ± 13	123 ± 11	207 ± 13	265 ± 14	200 ± 13	210 ± 13	229 ± 13	207 ± 13
Nb	96 ± 8	98 ± 8	128 ± 10	51 ± 6	102 ± 9	131 ± 10	94 ± 8	110 ± 9	119 ± 9	99 ± 9
Ba	59 ± 26	50 ± 27	-37	80 ± 26	-37	163 ± 25	122 ± 25	-38	-37	50 ± 26

Sample Number	49-2-549.0	49-2-559.0	49-2-569.0	49-2-581.5	49-2-596.0	49-2-606.5	49-2-615.2	49-2-625.5	49-2-637.2	49-2-647.0
Depth (ft.)	549.0	559.0	569.0	581.5	596.0	606.5	615.2	625.5	637.2	647.0
Strat. Unit	Qbt 1g	Qbt t	Qct	Qct	Qct	Qbo	Qbo	Qbo	Qbo	Qbo
XRF file	BRO275	BRO276	BRO276	BRO276						
Fusion Number	5113	5114	5115	5116	5117	5118	5119	5120	5121	5122

Major Elements (wt.%)

SiO ₂	76.1 ± 1.0	74.4 ± 1.0	73.9 ± 1.0	73.5 ± 0.9	78.8 ± 1.0	73.7 ± 0.9	73.1 ± 0.9	72.4 ± 0.9	72.2 ± 0.9	74.0 ± 1.0
TiO ₂	0.06 ± 0.02	0.06 ± 0.02	0.24 ± 0.01	0.26 ± 0.01	0.15 ± 0.01	0.28 ± 0.01	0.23 ± 0.01	0.22 ± 0.01	0.25 ± 0.01	0.15 ± 0.01
Al ₂ O ₃	11.2 ± 0.3	11.7 ± 0.3	12.1 ± 0.2	12.2 ± 0.2	10.0 ± 0.3	11.7 ± 0.3	12.5 ± 0.2	12.4 ± 0.2	12.4 ± 0.2	12.1 ± 0.2
Fe ₂ O ₃ T	1.43 ± 0.06	1.54 ± 0.06	2.02 ± 0.06	2.03 ± 0.06	1.51 ± 0.06	2.09 ± 0.06	2.07 ± 0.06	1.82 ± 0.06	2.27 ± 0.06	1.66 ± 0.06
MnO	0.08 ± 0.01	0.09 ± 0.01	0.08 ± 0.01	0.06 ± 0.01	0.05 ± 0.01	0.06 ± 0.01	0.06 ± 0.01	0.06 ± 0.01	0.07 ± 0.01	0.06 ± 0.01
MgO	-0.08	-0.08	0.40 ± 0.07	0.47 ± 0.07	0.28 ± 0.07	0.77 ± 0.07	0.56 ± 0.07	0.49 ± 0.07	0.71 ± 0.07	0.24 ± 0.07
CaO	0.27 ± 0.11	0.31 ± 0.11	0.69 ± 0.11	0.79 ± 0.11	0.62 ± 0.11	1.32 ± 0.10	1.03 ± 0.11	0.92 ± 0.11	1.06 ± 0.11	0.67 ± 0.11
Na ₂ O	3.88 ± 0.08	4.06 ± 0.09	2.89 ± 0.08	2.87 ± 0.08	3.12 ± 0.08	3.15 ± 0.08	3.61 ± 0.08	3.62 ± 0.08	3.64 ± 0.08	3.73 ± 0.08
K ₂ O	4.18 ± 0.05	4.28 ± 0.05	3.80 ± 0.05	3.94 ± 0.05	3.30 ± 0.04	3.69 ± 0.05	4.02 ± 0.05	4.10 ± 0.05	3.93 ± 0.05	4.29 ± 0.05
P ₂ O ₅	-0.01	-0.01	0.02 ± 0.01	0.03 ± 0.01	0.04 ± 0.01	0.06 ± 0.01	0.06 ± 0.01	0.04 ± 0.01	0.07 ± 0.01	0.03 ± 0.01
LOI %	1.87	2.57	2.98	3.05	1.25	2.09	2.30	2.56	2.53	2.22
Total	99.2	99.0	99.2	99.2	99.2	99.0	99.5	98.6	99.2	99.1

Trace Elements (ppm)

V	15 ± 7	-7	20 ± 8	22 ± 8	-7	23 ± 8	16 ± 7	13 ± 7	16 ± 8	8 ± 7
Cr	-8	-8	10 ± 8	11 ± 8	-8	15 ± 8	10 ± 8	13 ± 8	13 ± 8	-8
Ni	-6	-6	8 ± 6	14 ± 6	-6	-6	9 ± 6	-6	9 ± 6	-6
Zn	103 ± 12	118 ± 13	51 ± 8	54 ± 8	57 ± 9	41 ± 8	44 ± 8	50 ± 8	53 ± 8	58 ± 9
Rb	231 ± 7	252 ± 7	129 ± 6	136 ± 6	109 ± 6	127 ± 6	150 ± 6	154 ± 6	144 ± 6	167 ± 7
Sr	9 ± 5	11 ± 5	77 ± 5	92 ± 5	83 ± 5	187 ± 7	163 ± 6	148 ± 6	158 ± 6	87 ± 5
Y	82 ± 8	99 ± 9	40 ± 5	40 ± 5	40 ± 5	43 ± 5	40 ± 5	51 ± 5	46 ± 5	53 ± 6
Zr	217 ± 13	235 ± 13	244 ± 14	248 ± 14	123 ± 11	164 ± 12	178 ± 12	178 ± 12	184 ± 12	179 ± 12
Nb	105 ± 9	120 ± 9	47 ± 6	51 ± 6	43 ± 6	55 ± 6	72 ± 7	68 ± 7	72 ± 7	76 ± 7
Ba	-37	-38	230 ± 24	269 ± 24	189 ± 24	285 ± 25	244 ± 24	192 ± 24	229 ± 24	167 ± 25

Sample Number	49-2-656.5	49-2-666.5	49-2-676.6	49-2-688.0
Depth (ft.)	656.5	666.5	676.6	688.0
Strat. Unit	Qbo	Qbo	Qbo	Qbo
XRF file	BRO276	BRO276	BRO276	BRO276
Fusion Number	5123	5124	5125	5126
<u>Major Elements (wt. %)</u>				
SiO ₂	74.5 ± 1.0	73.9 ± 1.0	73.6 ± 0.9	74.8 ± 1.0
TiO ₂	0.16 ± 0.01	0.16 ± 0.01	0.16 ± 0.01	0.05 ± 0.02
Al ₂ O ₃	12.1 ± 0.2	12.1 ± 0.2	12.1 ± 0.2	11.9 ± 0.3
Fe ₂ O ₃ T	1.84 ± 0.06	1.82 ± 0.06	1.89 ± 0.06	1.40 ± 0.06
MnO	0.07 ± 0.01	0.08 ± 0.01	0.08 ± 0.01	0.09 ± 0.01
MgO	0.26 ± 0.07	0.28 ± 0.07	0.28 ± 0.07	-0.08
CaO	0.72 ± 0.11	0.73 ± 0.11	0.75 ± 0.11	0.20 ± 0.11
Na ₂ O	3.89 ± 0.08	3.82 ± 0.08	3.86 ± 0.08	3.82 ± 0.08
K ₂ O	4.02 ± 0.05	4.01 ± 0.05	4.01 ± 0.05	4.65 ± 0.05
P ₂ O ₅	0.04 ± 0.01	0.04 ± 0.01	0.04 ± 0.01	-0.01
LOI %	2.22	2.18	2.16	2.48
Total	99.9	99.1	98.9	99.3
<u>Trace Elements (ppm)</u>				
V	12 ± 7	13 ± 7	8 ± 7	-7
Cr	-8	-8	-8	-8
Ni	-6	-6	-6	-6
Zn	85 ± 10	83 ± 10	89 ± 11	110 ± 12
Rb	233 ± 7	252 ± 7	248 ± 7	345 ± 9
Sr	87 ± 5	83 ± 6	86 ± 5	-5
Y	83 ± 7	77 ± 8	80 ± 8	99 ± 9
Zr	213 ± 13	217 ± 13	211 ± 13	253 ± 14
Nb	116 ± 9	125 ± 10	122 ± 9	179 ± 12
Ba	172 ± 24	185 ± 24	213 ± 24	-37

Appendix B

INAA Results for Borehole 49-2-700-1

Appendix B. INAA Results for Borehole 49-2-700-1

Lab Number	49-2-023	49-2-033	49-2-043	49-2-053	49-2-063	49-2-073	49-2-083
Unit Designation	Qbt 4						
Fe (%)	1.71	1.85	1.6	1.61	1.55	1.5	1.6
cv%	0.8	0.7	0.7	0.7	0.7	0.8	0.7
CaO (%)	0.672	0.658	0.374	0.762	0.252	0.34	0.392
cv%	18.6	18.5	19.2	18.4	22.6	22	19.1
Na ₂ O (%)	3.22	3.08	3.24	3.3	3.28	3.33	3.13
cv%	0.7	0.7	0.7	0.8	0.8	0.8	0.8
K ₂ O (%)	3.64	3.51	3.5	3.64	3.79	3.77	3.27
cv%	6.7	6.8	8	8.3	7.2	8.5	9
Rb (ppm)	78.8	90.9	76.2	83.1	82.4	85.7	86.6
cv%	4	3.8	3.9	4	3.5	3.3	3.7
Sr (ppm)	87	111	106	103	88.7	90.3	125
cv%	9.5	15.2	9.2	9.6	6.8	8.4	7.8
Cs (ppm)	1.97	2.63	1.76	1.8	1.79	1.72	1.74
cv%	2.1	1.6	2	2	2	2	2.3
Ba (ppm)	376	363	396	353	347	285	351
cv%	3.7	3.4	3.3	3.8	3.8	3.7	3.8
Th (ppm)	11.8	11.6	10.9	11.6	11.4	12.2	10.5
cv%	0.9	0.9	0.9	0.9	0.8	0.8	0.9
U (ppm)	3.43	3.32	3.11	3.26	3.24	3.39	3.3
cv%	2.2	2.2	2.1	2.2	2.2	2.3	2.4
La (ppm)	65.8	61.6	63.1	65.8	64	67.8	50.9
cv%	0.5	0.5	0.5	0.5	0.5	0.5	0.5
Ce (ppm)	126	120	121	128	125	133	99.3
cv%	0.7	0.7	0.7	0.7	0.7	0.7	0.8
Nd (ppm)	48.5	46.3	46.7	49.5	46.4	51.7	39.2
cv%	2.8	2.8	2.5	2.8	2.6	2.7	2.9
Sm (ppm)	9.25	8.92	8.75	9.13	8.9	9.35	7.73
cv%	0.5	0.5	0.5	0.5	0.5	0.5	0.5
Eu (ppm)	0.601	0.67	0.64	0.58	0.581	0.494	0.483
cv%	2	1.9	1.7	1.9	1.9	2	2.2
Gd (ppm)	7.2	7.35	7.15	7.28	7.4	7.36	6.57
cv%	3.9	3.6	3.9	4.1	4	3.9	3.7
Tb (ppm)	1.07	1.06	1.01	1.05	1.03	1.1	0.989
cv%	1.3	1.4	1.3	1.4	1.3	1.3	1.5
Ho (ppm)	1.42	1.39	1.32	1.5	1.4	1.43	1.39
cv%	9.1	9.1	9.7	10.7	10.4	9.7	10.4

Note: cv% = coefficient of variance (computed based on a one-sigma uncertainty in counting statistics); given as a relative percent of reported value.

Lab Number	49-2-023	49-2-033	49-2-043	49-2-053	49-2-063	49-2-073	49-2-083
Unit Designation	Qbt 4						
Tm (ppm)	0.603	0.595	0.543	0.598	0.597	0.635	0.556
cv%	5.4	5.3	5.8	5.6	5.5	4.8	5.6
Yb (ppm)	3.68	3.63	3.39	3.69	3.62	3.82	3.38
cv%	2.2	2.1	2.1	2	2	2	2.3
Lu (ppm)	0.511	0.493	0.46	0.501	0.512	0.506	0.45
cv%	2.1	2	2.5	2	1.9	2.6	2.1
Zr (ppm)	345	323	340	339	329	340	240
cv%	3.5	3.3	3.1	3	3	2.9	4.4
Hf (ppm)	8.7	8.33	8.38	8.78	8.49	8.85	6.46
cv%	1	1	0.9	0.9	0.9	0.9	1.1
Ta (ppm)	2.99	2.86	2.82	3.02	3	4.74	5.26
cv%	0.7	0.7	0.6	0.7	0.6	0.6	0.5
W (ppm)	437	396	392	467	426	408	678
cv%	1.1	1.1	1.1	1.1	1.1	1.1	1
Sc (ppm)	3.26	4.51	3.3	3.15	3.05	2.78	3.27
cv%	0.8	0.7	0.8	0.8	0.8	0.8	0.8
Cr (ppm)	5.07	9.88	5.81	3.54	3.87	2.25	12.4
cv%	5.7	3.9	6.3	7.8	8.4	7.5	3.4
Co (ppm)	41.1	36.6	36.4	44.2	41.3	30.5	61.2
cv%	0.7	0.7	0.7	0.7	0.7	0.7	0.7
Ni (ppm)	<2.96	9.34	9.12	12.8	145	16.7	20
cv%	60	17.7	17.7	12.6	17.2	20.4	16
Zn (ppm)	62.1	71.7	61.6	65.4	61.6	64.3	101
cv%	3.1	2.7	3	3.3	3.2	3.1	2.5
As (ppm)	1.48	1.3	1.06	0.818	0.887	1.09	0.981
cv%	9.4	9.1	10.5	16	16	9.6	10.3
Sb (ppm)	0.247	0.199	0.13	0.159	0.172	0.126	0.219
cv%	10	11.7	14	13.4	11.9	13.5	9.5
Au (ppb)	2.71	<1.51	<0.979	3.55	<1.02	<0.966	3.26
cv%	18.5	60	60	16	60	60	13.3

Lab Number	49-2-093	49-2-103	49-2-126	49-2-136	49-2-156	49-2-179
Unit Designation	Qbt 3					
Fe (%)	1.09	1.11	1.06	0.951	0.91	0.638
cv%	0.8	0.8	0.8	0.8	0.9	1.1
CaO (%)	0.542	0.449	0.491	0.399	0.307	0.156
cv%	18.6	18.9	18.8	18.9	22	25.9
Na ₂ O (%)	3.12	3.1	3.09	2.95	2.83	2.45
cv%	0.8	0.8	0.8	0.8	0.8	0.8
K ₂ O (%)	3.94	3.76	3.31	3.08	3.37	2.92
cv%	7.6	7.6	8.9	10.7	10.7	10.6
Rb (ppm)	92.6	100	95.8	86.5	83.1	54.8
cv%	3.4	3	3.1	3.3	4.1	4.8
Sr (ppm)	53.4	42.3	53	52.1	41.6	55
cv%	12.4	11.8	12.4	12.1	23	13.7
Cs (ppm)	1.86	1.82	1.88	1.58	1.34	0.89
cv%	2	1.9	1.9	2	2.5	3.5
Ba (ppm)	188	212	192	159	183	149
cv%	5.2	5.2	6.3	6	7.6	6.1
Th (ppm)	12.5	12.7	12.2	10.8	10.3	6.01
cv%	0.8	0.8	0.8	0.8	0.9	1.1
U (ppm)	3.7	3.86	3.66	3.12	3.1	1.89
cv%	2.2	2.2	2.1	2.2	2.6	3.9
La (ppm)	55.2	56.4	54	49	45.5	25.3
cv%	0.5	0.5	0.5	0.5	0.5	0.6
Ce (ppm)	111	111	108	96.8	89.7	50.5
cv%	0.7	0.7	0.7	0.8	0.8	1
Nd (ppm)	42.4	42.4	39.7	38.3	33.3	19.4
cv%	2.8	2.9	3	3.2	4.1	6.3
Sm (ppm)	8.33	8.63	8.2	7.18	7.03	3.98
cv%	0.5	0.6	0.5	0.5	0.5	0.6
Eu (ppm)	0.276	0.271	0.269	0.275	0.251	0.224
cv%	2.7	2.7	2.9	2.8	3.3	3.6
Gd (ppm)	7.23	7.31	7.32	6.2	5.91	3.49
cv%	3.9	3.4	3.4	4.2	4.4	5.8
Tb (ppm)	1.09	1.11	1.06	0.921	0.922	0.54
cv%	1.3	1.3	1.3	1.4	1.4	1.9
Ho (ppm)	1.46	1.47	1.45	1.24	1.26	0.738
cv%	10.4	11	9.3	9.1	9.8	12.3
Tm (ppm)	0.63	0.609	0.596	0.526	0.535	0.305
cv%	4.9	5.2	5	5.2	5.6	7.4
Yb (ppm)	3.77	3.89	3.82	3.28	3.17	1.87

Lab Number	49-2-093	49-2-103	49-2-126	49-2-136	49-2-156	49-2-179
Unit Designation	Qbt 3					
cv%	1.9	1.9	1.9	1.9	2.8	4.1
Lu (ppm)	0.508	0.518	0.532	0.464	0.438	0.263
cv%	1.9	1.9	3	1.9	2	2.7
Zr (ppm)	256	252	228	214	205	99.2
cv%	3.2	3.2	3.9	3.9	4.3	7.7
Hf (ppm)	7.18	7.27	6.81	5.98	5.81	3.28
cv%	1	1	1	1	1.1	1.5
Ta (ppm)	3.46	5.89	3.37	5.71	6.86	7.63
cv%	0.6	0.5	0.6	0.5	0.5	0.5
W (ppm)	743	591	809	777	1090	1590
cv%	1	1	1	1	1	1
Sc (ppm)	1.7	1.73	1.62	1.59	1.54	1.01
cv%	0.9	0.9	0.9	0.9	0.9	1
Cr (ppm)	1.74	1.38	1.99	1.52	0.409	2.46
cv%	13.3	14.8	14.1	14.2	19.7	7.1
Co (ppm)	70.4	46.6	66.2	52.4	109	137
cv%	0.7	0.7	0.7	0.7	0.6	0.6
Ni (ppm)	6.45	7.12	6.76	4.98	6.85	7.07
cv%	24.8	21.9	23.3	23.3	19.6	18.7
Zn (ppm)	58.7	46.8	56.3	42.2	35.8	24.2
cv%	3.6	2.4	3.3	2.5	2.9	7.6
As (ppm)	0.885	0.523	0.481	0.38	0.589	2.84
cv%	15.4	15.7	17.8	18	17.7	21.1
Sb (ppm)	0.133	0.243	0.139	0.13	0.135	0.0834
cv%	14.6	9.1	13.8	13.5	10.4	14.5
Au (ppb)	1.14	1.82	1.38	1.04	<0.798	<0.326
cv%	23.4	17.8	20.8	20.8	60	60

Lab Number	49-2-189	49-2-197	49-2-206	49-2-227	49-2-247	49-2-267	49-2-287	49-2-307
Unit Designation	Qbt 2							
Fe (%)	0.933	0.906	0.976	1.03	1.05	1.01	1.12	1.06
cv%	0.8	0.9	0.8	0.8	0.8	0.9	0.6	0.7
CaO (%)	0.269	0.122	0.148	0.123	0.138	0.134	0.278	0.694
cv%	24.8	26.5	26.3	26.3	26.6	26.4	19.9	20.1
Na ₂ O (%)	2.93	2.94	3.04	3.01	3.08	3.03	3.08	2.95
cv%	0.8	0.8	0.8	0.8	0.8	0.8	0.9	0.7
K ₂ O (%)	2.94	3.62	3.47	4.52	5.32	3.85	3.68	3.11
cv%	9.8	10.5	10.9	10.7	10.3	10.8	13.2	7.9
Rb (ppm)	120	121	135	128	137	131	149	184
cv%	2.7	2.5	2.4	2.3	2.5	2.6	2.4	1.4
Sr (ppm)	20.7	29.7	24.1	40.2	32.5	21.9	54.7	39.6
cv%	16.4	24.7	24.8	16	19.5	28.7	10.8	21.6
Cs (ppm)	2.83	2.51	2.78	2.52	3.05	2.61	3.59	4.57
cv%	1.6	1.6	1.5	1.4	1.5	1.8	1	1
Ba (ppm)	140	111	74.9	120	101	104	120	78.4
cv%	6.9	6.9	8	6.4	7.1	6.9	5.7	4.3
Th (ppm)	14.6	14.4	16.7	15.7	16.6	16	17.5	21
cv%	0.8	0.8	0.8	0.7	0.8	0.8	0.6	0.6
U (ppm)	4.47	4.32	5.06	4.75	5.01	5.05	5.62	7.34
cv%	2	1.9	1.9	1.7	1.9	1.8	1.7	1.4
La (ppm)	51.6	50.3	56.2	54.5	56.6	53.6	54.8	47.4
cv%	0.5	0.5	0.5	0.5	0.5	0.5	0.5	0.5
Ce (ppm)	106	99.4	113	108	113	109	111	105
cv%	0.8	0.8	0.8	0.7	0.8	0.9	0.6	1.1
Nd (ppm)	39.8	38.4	43.7	40.4	43.1	42.4	45.1	44.6
cv%	3.6	3.5	2.6	2.5	3.1	3	2.5	1.6
Sm (ppm)	8.5	8.54	9.91	9.07	9.7	9.37	10.3	11.5
cv%	0.5	0.5	0.5	0.5	0.5	0.5	0.5	0.7
Eu (ppm)	0.156	0.151	0.135	0.153	0.176	0.157	0.175	0.111
cv%	3.8	3.9	4.1	3.5	3.6	3.7	2.5	4.4
Gd (ppm)	8.35	8.44	9.41	9.33	9.08	9.14	9.94	12.1
cv%	3.5	5.1	3.7	4.5	3.5	3.3	3.2	4.3
Tb (ppm)	1.27	1.25	1.46	1.39	1.45	1.41	1.57	1.97
cv%	1.1	1.2	1.1	1	1.1	1.2	0.8	0.8
Ho (ppm)	1.69	1.7	2.01	1.91	2.02	1.97	2.2	2.85
cv%	8.1	7.1	7.8	7.1	7.8	6.9	7.5	6.7
Tm (ppm)	0.74	0.736	0.849	0.837	0.834	0.851	0.93	1.13
cv%	4.6	4.2	4	3.9	4.2	4.1	4	3.8
Yb (ppm)	4.54	4.42	5.33	4.97	5.16	5.2	5.73	7.16

Lab Number	49-2-189	49-2-197	49-2-206	49-2-227	49-2-247	49-2-267	49-2-287	49-2-307
Unit Designation	Qbt 2							
cv%	1.7	1.6	1.6	1.5	1.5	1.6	1.3	1
Lu (ppm)	0.591	0.577	0.725	0.69	0.698	0.69	0.816	0.994
cv%	2.1	2	1.9	1.7	2	1.8	1.5	0.9
Zr (ppm)	213	203	223	206	229	222	218	248
cv%	3.7	3.5	3.9	3.5	3.8	3.6	2.5	3.3
Hf (ppm)	6.77	6.56	7.45	7	7.29	7.23	7.32	8.34
cv%	1	1	1	0.9	1	1.1	0.8	0.7
Ta (ppm)	7.07	6.76	5.08	6.33	4.89	4.83	5.32	8.98
cv%	0.5	0.5	0.5	0.5	0.6	0.6	0.5	0.4
W (ppm)	738	668	638	443	618	627	545	556
cv%	1	1	1.1	1.1	1.1	1.1	1.1	1.4
Sc (ppm)	1.22	1.12	1.15	1.3	1.47	1.26	1.55	1.13
cv%	0.9	0.9	0.9	0.9	0.9	1	0.7	0.8
Cr (ppm)	1.44	1.26	1.13	1.19	1.59	1.77	2.34	2.33
cv%	15.6	16	15.5	13.8	14.2	14	6.3	6.3
Co (ppm)	52.1	60.1	49	34	54.2	52.9	34.3	49.4
cv%	0.7	0.7	0.7	0.7	0.7	0.9	0.6	0.6
Ni (ppm)	5.96	5.19	6.28	6.18	6.17	10.3	3.14	3.66
cv%	20.8	23.4	23.4	19.7	19.8	15.6	25.3	23.7
Zn (ppm)	35.8	45.6	53.7	57.7	55.5	59.5	73.9	76.5
cv%	3.6	3.2	2.9	2.3	2.8	2.4	1.8	1.9
As (ppm)	0.822	0.449	0.932	0.774	0.877	0.444	1.15	0.871
cv%	14.9	18	11.6	14.4	16.2	20.9	14.9	13.7
Sb (ppm)	0.117	0.102	0.185	0.155	0.135	0.176	0.183	0.188
cv%	13.8	16.3	11.5	9.9	14	12	7.2	8.2
Au (ppb)	1	2.85	1.29	0.736	<0.351	<0.332	1.37	<0.316
cv%	25.1	13.9	23.5	22.3	60	60	15	60

Lab Number	49-2-322	49-2-342	49-2-365	49-2-385	49-2-405	49-2-425	49-2-458	49-2-485	49-2-496
Unit Designation	Qbt 1v	Qbt 1v	Qbt 1v	Qbt 1g					
Fe (%)	0.974	0.966	1.06	1.03	1.19	1.05	1.09	0.964	1.34
cv%	0.8	0.7	0.7	0.7	0.7	0.7	0.8	0.8	0.7
CaO (%)	0.931	0.585	<0.272	0.508	<0.31	0.287	0.308	<0.306	0.677
cv%	18.2	22.6	51	24	51	29.9	29.9	51	22.5
Na ₂ O (%)	2.82	2.85	2.95	2.84	2.63	2.78	2.83	2.79	2.91
cv%	0.8	0.8	0.8	0.8	0.8	0.8	0.8	0.8	0.8
K ₂ O (%)	3.12	2.79	3.1	3.34	4	3	3.21	2.91	3.16
cv%	8.9	8.9	9.1	7.9	9.3	10	10	11.8	9.5
Rb (ppm)	178	175	182	196	245	209	254	215	263
cv%	1.6	1.5	1.4	1.5	1.5	1.4	1.3	1.5	1.3
Sr (ppm)	37.4	34.2	45.4	48.3	39.2	29.8	24	22.1	81.9
cv%	24.6	26.5	13.8	20.4	19.5	18.6	21.9	18	12.4
Cs (ppm)	4.44	5.41	4.85	7.26	10.2	8.01	8.94	6.99	9.1
cv%	1.3	1	1.1	0.9	0.9	0.9	0.9	1	0.9
Ba (ppm)	92.2	80.3	107	103	104	78.9	64.2	34.5	151
cv%	5.6	5.5	4.1	4.8	5	4.8	5.9	8	3.4
Th (ppm)	20.7	20.9	21.8	22.3	25.8	24.2	30.3	25.3	31.4
cv%	0.6	0.6	0.6	0.6	0.6	0.6	0.5	0.6	0.5
U (ppm)	7.13	7.27	7.59	8	9.49	8.43	11.1	9	11.3
cv%	1.5	1.5	1.5	1.4	1.4	1.4	1.3	1.5	1.3
La (ppm)	44.3	45.8	47.7	47.6	50	48.9	53.4	46.9	57
cv%	0.6	0.6	0.5	0.5	0.6	0.5	0.5	0.6	0.5
Ce (ppm)	98.7	101	103	102	110	100	117	102	130
cv%	1.2	1.2	1.2	1.2	1.2	1.2	1.2	1.3	1.1
Nd (ppm)	42.2	41.2	44.4	42.3	45.8	41.8	45.7	42.4	48.7
cv%	1.7	1.7	1.5	1.7	1.7	1.7	1.7	1.8	1.8
Sm (ppm)	10.9	10.8	11.3	11.4	12.7	11.4	13.2	11.5	13.3
cv%	0.7	0.7	0.7	0.7	0.7	0.7	0.7	0.7	0.7
Eu (ppm)	0.118	0.108	0.139	0.115	0.105	0.108	0.0857	0.0693	0.183
cv%	5	4.7	4	4.5	6.2	5	8.7	7.2	4
Gd (ppm)	11.7	11.3	11.9	11.3	13.6	12.1	14.5	11.9	15.9
cv%	5.2	4.7	4.7	4.5	3.1	3.6	4.5	3.8	3.6
Tb (ppm)	1.92	1.9	1.97	1.94	2.25	2.05	2.47	2.07	2.68
cv%	0.9	0.8	1	0.9	0.9	0.8	0.8	0.9	0.8
Ho (ppm)	2.66	2.68	2.73	2.79	3.3	2.9	3.6	2.98	3.93
cv%	7.3	8.4	7.5	7.9	8	8.3	6.2	8.8	5.3
Tm (ppm)	1.16	1.14	1.16	1.19	1.49	1.29	1.62	1.43	1.75
cv%	3.8	3.7	3.6	4	3.7	3.6	3.3	3.6	3.1
Yb (ppm)	6.99	7.04	7.34	7.53	8.81	8.04	10.4	8.41	11

Lab Number	49-2-322	49-2-342	49-2-365	49-2-385	49-2-405	49-2-425	49-2-458	49-2-485	49-2-496
Unit Designation	Qbt 1v	Qbt 1v	Qbt 1v	Qbt 1g					
cv%	1.1	1.1	1	1	1	1	0.9	1	0.9
Lu (ppm)	1	0.991	1.07	1.07	1.24	1.12	1.44	1.19	1.53
cv%	0.9	1	1	1	0.9	0.9	0.8	1	0.8
Zr (ppm)	221	231	236	227	259	243	291	241	306
cv%	4.9	3.5	3.1	4.2	3.5	3.5	3.6	4	4
Hf (ppm)	8.11	8.18	8.38	8.62	10	9.07	11.5	9.63	12.2
cv%	0.8	0.7	0.7	0.7	0.7	0.7	0.7	0.7	0.7
Ta (ppm)	11.1	6.93	9.97	7.54	8.86	11.3	10.6	14.1	13.3
cv%	0.4	0.4	0.4	0.4	0.4	0.4	0.4	0.4	0.4
W (ppm)	1040	1050	709	718	993	808	641	1270	599
cv%	1	1	1	1	1	1	1	1	1
Sc (ppm)	1.07	1.17	1.27	1.19	1.14	1.13	0.859	0.817	1.59
cv%	0.9	0.8	0.8	0.8	0.8	0.8	0.9	1	0.7
Cr (ppm)	3.31	3.67	3.68	3.12	2.92	2.35	1.42	1.39	6.27
cv%	8.1	9.3	7	7.4	8.4	11.6	16.1	14.3	4.6
Co (ppm)	153	82.3	58.6	93.1	159	83	126	152	136
cv%	0.5	0.5	0.6	0.5	0.5	0.5	0.5	0.5	0.5
Ni (ppm)	3.88	4.82	6.97	6.78	2.43	5.23	4.82	5.83	8.92
cv%	17.1	16.7	23.3	20.9	27.6	16.1	25.2	18	13.3
Zn (ppm)	62.1	62.6	176	86	56.9	74.9	109	87.9	263
cv%	3.4	2.4	1.4	2	2.9	2.3	2	2.7	1.3
As (ppm)	0.53	1.95	1.49	2.14	2.03	1.71	2.69	2.12	3.72
cv%	16.9	8	8.5	6.6	7.9	8.2	6.8	8	5.7
Sb (ppm)	0.226	0.409	0.253	0.298	0.377	0.348	0.422	0.4	0.437
cv%	11	5.4	7.2	7.2	7.9	6.6	6.3	6.8	7
Au (ppb)	0.579	0.357	1.65	2.36	5.1	2.53	1.85	3.01	2.83
cv%	27.4	27.9	24.9	17.8	14.3	15.7	18.8	17.7	17.8

Lab Number	49-2-516	49-2-539	49-2-559	49-2-569	49-2-606	49-2-625	49-2-647	49-2-666	49-2-688
Unit Designation	Qbt 1g	Qbt 1g	Qbt t	Qct	Qbo	Qbo	Qbo	Qbo	Qbo
Fe (%)	0.997	0.985	1.04	1.41	1.61	1.5	1.16	1.26	0.98
cv%	0.7	0.7	0.7	0.6	0.6	0.7	0.7	0.6	0.8
CaO (%)	0.373	0.3	0.396	0.686	0.833	0.715	0.328	0.705	0.387
cv%	24.2	29.9	29.6	12.3	12	21.3	29.9	21.2	29.9
Na ₂ O (%)	2.85	2.82	2.91	2.16	2.33	2.7	2.75	2.91	2.88
cv%	0.8	0.8	0.8	0.9	0.9	0.9	0.9	0.9	0.9
K ₂ O (%)	3.71	3.39	3.01	2.81	2.87	3.2	3.65	3.82	3.7
cv%	9.9	10.3	13.4	10.2	11.1	12.7	12.2	10.8	13.1
Rb (ppm)	226	225	246	129	130	156	167	246	344
cv%	1.3	1.2	1.3	1.4	1.6	1.9	1.7	1.1	1.2
Sr (ppm)	35.9	34.9	37.1	103	204	158	111	101	24.2
cv%	21.7	24.7	21.7	8.8	6.1	9.4	9.2	7.9	23.4
Cs (ppm)	7.35	7.36	8.28	10.4	3.33	4.25	4.22	7.21	10.5
cv%	0.9	0.9	0.9	0.8	1.4	1.5	1.2	0.9	0.9
Ba (ppm)	32.6	41.8	30.3	231	290	220	182	192	57.2
cv%	7.6	7.2	8.4	2.2	2.1	3	2.7	2.5	7.2
Th (ppm)	26.3	26.4	28.9	15.4	15.2	19.4	20.7	31	44.4
cv%	0.5	0.5	0.5	0.6	0.6	0.6	0.6	0.5	0.5
U (ppm)	9.47	9.29	10.3	5.06	5.56	7.42	7.96	12.5	18.4
cv%	1.3	1.3	1.3	1.5	1.6	1.4	1.4	1.1	1.1
La (ppm)	49.5	49.8	52.9	42.3	39.3	42.1	43.5	41.2	41.8
cv%	0.5	0.6	0.5	0.5	0.6	0.6	0.6	0.6	0.6
Ce (ppm)	105	108	110	81.1	76.8	86	89.2	92.5	98.6
cv%	1.1	1.2	1.2	1.2	1.3	1.3	1.2	1.2	1.3
Nd (ppm)	42.9	43.7	46.7	34	31.7	36.5	37.5	42.3	46.5
cv%	1.6	1.8	1.7	1.8	2	2	1.8	1.6	1.9
Sm (ppm)	11.7	11.5	12.6	7.18	6.93	8.38	8.66	11.7	14.2
cv%	0.7	0.7	0.7	0.7	0.8	0.7	0.7	0.7	0.7
Eu (ppm)	0.0666	0.0698	0.0726	0.46	0.429	0.323	0.209	0.244	0.0302
cv%	6.5	6	7.6	1.7	2	3.5	3.1	2.5	15.6
Gd (ppm)	13	12.9	13.8	6.54	6.7	8.09	8.9	12	16.2
cv%	4.6	3.1	3.3	4.1	4	4.9	5.4	3.6	4.8
Tb (ppm)	2.21	2.18	2.34	1.01	1.06	1.35	1.36	2.02	2.67
cv%	0.8	0.8	0.8	1	1.2	1.3	1	0.8	0.9
Ho (ppm)	3.32	3.18	3.5	1.47	1.51	1.87	1.94	2.94	3.87
cv%	5.6	6.2	5.9	8	10.4	8	8.8	6.7	5.9
Tm (ppm)	1.44	1.43	1.56	0.664	0.686	0.793	0.843	1.28	1.74
cv%	3.5	3.3	3.5	4.6	5.8	4.8	4.8	3.6	3.4
Yb (ppm)	8.84	8.94	9.61	4.11	4.09	5.01	5.31	8	11.2

Lab Number	49-2-516	49-2-539	49-2-559	49-2-569	49-2-606	49-2-625	49-2-647	49-2-666	49-2-688
Unit Designation	Qbt 1g	Qbt 1g	Qbt t	Qct	Qbo	Qbo	Qbo	Qbo	Qbo
cv%	0.9	1	1	1.2	1.4	1.5	1.2	1	1
Lu (ppm)	1.24	1.24	1.34	0.596	0.574	0.718	0.759	1.11	1.54
cv%	0.8	0.8	0.9	1	1.2	1.1	1.1	0.9	0.9
Zr (ppm)	257	242	273	255	173	183	209	240	285
cv%	4	4.2	3.6	3.5	5	6.4	4.5	3.2	3.8
Hf (ppm)	10	10.1	10.9	7.68	5.59	6.73	6.98	9.38	12.8
cv%	0.7	0.7	0.7	0.7	0.8	0.9	0.8	0.7	0.7
Ta (ppm)	12.1	9.29	10.2	4.97	4.97	8.54	7.23	12.6	17.5
cv%	0.4	0.4	0.4	0.4	0.5	0.4	0.4	0.4	0.4
W (ppm)	803	987	818	211	857	547	720	275	504
cv%	1	1	1	1.1	1	1	1	1.1	1
Sc (ppm)	0.859	0.82	0.838	3.54	4.02	3.21	1.93	1.87	0.603
cv%	0.9	0.9	0.9	0.6	0.6	0.7	0.7	0.7	1.2
Cr (ppm)	1.28	3.41	1.28	12.6	17.9	14.3	4.04	4.24	1.66
cv%	12.9	10.1	14.4	1.9	1.9	3.5	5.5	5.1	16.8
Co (ppm)	123	92.5	111	18	79.4	282	68.2	24.6	167
cv%	0.5	0.5	0.5	0.6	0.5	0.5	0.5	0.6	0.5
Ni (ppm)	6.88	7.9	12.2	4.85	7.48	17.3	3.18	6.47	5.87
cv%	20.2	22.4	13.3	22.8	14.6	18.4	26.4	17.2	25.2
Zn (ppm)	101	97.2	103	55.8	62.5	68.6	50.5	74.6	99.1
cv%	2	1.9	2	2.5	2.9	3	2.3	2	2.3
As (ppm)	2.09	2.13	2.34	1.74	1.11	1.57	1.9	2.71	3.98
cv%	9.9	8.9	7.7	8.1	14.4	11.8	10.5	8.2	7.2
Sb (ppm)	0.376	0.396	0.41	0.416	0.205	0.248	0.241	0.415	0.594
cv%	7.1	6	6.2	4.6	9.4	12.1	8.2	5.2	5.9
Au (ppb)	0.569	1.96	0.665	<0.725	2.31	<0.803	1.43	<0.1	1.63
cv%	23	22	25.8	60	19.5	60	19	0	22.4

Appendix C

Bulk-Tuff Mineralogy for Borehole 49-2-700-1

Appendix C. Bulk-Tuff Mineralogy for Borehole 49-2-700-1

Location ID	Depth (ft)	Stratigraphic Unit	Smectite	Tridymite	Cristobalite	Quartz	Feldspar	Glass	Hematite	Mica	Hornblende
TA-49	7.1	Qf-Qmt	2 ± 1	–	23 ± 2	9 ± 1	64 ± 9	–	2 ± 1	Tr	Tr
TA-49	23.1	Qbt 4	2 ± 1	1 ± 1	19 ± 1	10 ± 1	68 ± 10	–	–	Tr	–
TA-49	33.0	Qbt 4	2 ± 1	6 ± 1	12 ± 1	10 ± 1	65 ± 9	–	–	–	–
TA-49	43.0	Qbt 4	1 ± 1	9 ± 1	11 ± 1	8 ± 1	67 ± 9	–	Tr	–	–
TA-49	53.0	Qbt 4	1 ± 1	1 ± 1	11 ± 1	8 ± 1	66 ± 9	–	–	Tr	–
TA-49	63.0	Qbt 4	1 ± 1	8 ± 1	12 ± 1	8 ± 1	67 ± 9	–	Tr	–	–
TA-49	73.0	Qbt 4	–	11 ± 1	11 ± 1	7 ± 1	69 ± 10	–	–	–	–
TA-49	83.7	Qbt 4	2 ± 1	13 ± 1	3 ± 1	17 ± 1	63 ± 9	–	Tr	Tr	–
TA-49	93.0	Qbt 3	–	16 ± 2	5 ± 2	18 ± 1	63 ± 9	–	–	–	–
TA-49	103.0	Qbt 3	–	11 ± 1	8 ± 3	12 ± 1	66 ± 9	–	–	–	–
TA-49	115.0	Qbt 3	–	12 ± 1	7 ± 3	17 ± 1	66 ± 9	–	–	–	–
TA-49	126.0	Qbt 3	Tr	19 ± 2	4 ± 2	18 ± 1	61 ± 9	–	–	–	–
TA-49	136.7	Qbt 3	Tr	20 ± 2	1 ± 1	22 ± 2	58 ± 8	–	–	–	–
TA-49	145.0	Qbt 3	–	20 ± 2	1 ± 1	20 ± 2	59 ± 8	–	–	–	–
TA-49	156.0	Qbt 3	–	18 ± 2	1 ± 1	20 ± 2	65 ± 9	–	–	–	–
TA-49	166.9	Qbt 3	–	19 ± 2	1 ± 1	20 ± 2	63 ± 9	–	–	Tr	–
TA-49	179.0	Qbt 3	–	9 ± 1	1 ± 1	42 ± 2	52 ± 7	–	–	Tr	–
TA-49	189.1	Qbt 2	–	19 ± 2	2 ± 1	22 ± 2	55 ± 8	–	Tr	–	–
TA-49	197.6	Qbt 2	Tr	19 ± 2	3 ± 1	19 ± 1	57 ± 8	–	Tr	–	–
TA-49	206.8	Qbt 2	Tr	18 ± 2	5 ± 2	17 ± 1	60 ± 8	–	Tr	–	–
TA-49	217.0	Qbt 2	–	22 ± 2	3 ± 1	18 ± 1	61 ± 9	–	Tr	–	–
TA-49	227.3	Qbt 2	1 ± 1	24 ± 2	2 ± 1	16 ± 1	60 ± 8	–	Tr	–	–
TA-49	237.0	Qbt 2	1 ± 1	20 ± 2	3 ± 1	19 ± 1	57 ± 8	–	Tr	–	–
TA-49	247.0	Qbt 2	Tr	19 ± 2	4 ± 2	15 ± 1	61 ± 9	–	1 ± 1	–	–
TA-49	257.0	Qbt 2	1 ± 1	20 ± 2	3 ± 1	19 ± 1	59 ± 8	–	Tr	–	Tr
TA-49	267.0	Qbt 2	Tr	19 ± 2	2 ± 1	16 ± 1	63 ± 9	–	1 ± 1	Tr	Tr
TA-49	277.3	Qbt 2	1 ± 1	19 ± 2	3 ± 1	19 ± 1	60 ± 8	–	1 ± 1	Tr	–
TA-49	287.0	Qbt 2	Tr	17 ± 2	3 ± 1	17 ± 1	62 ± 9	–	1 ± 1	–	Tr
TA-49	297.0	Qbt 2	–	18 ± 2	4 ± 2	15 ± 1	61 ± 9	–	1 ± 1	–	–
TA-49	307.0	Qbt 2	Tr	10 ± 1	9 ± 4	18 ± 1	61 ± 9	–	Tr	Tr	–
TA-49	322.7	Qbt 1v	Tr	6 ± 1	12 ± 1	21 ± 2	59 ± 8	–	1 ± 1	–	Tr
TA-49	332.2	Qbt 1v	Tr	3 ± 1	19 ± 1	19 ± 1	59 ± 8	–	1 ± 1	Tr	Tr
TA-49	342.0	Qbt 1v	–	–	19 ± 1	23 ± 2	55 ± 8	–	Tr	–	Tr
TA-49	355.2	Qbt 1v	–	–	21 ± 2	21 ± 2	56 ± 8	–	1 ± 1	–	Tr
TA-49	365.2	Qbt 1v	–	2 ± 1	21 ± 2	18 ± 1	58 ± 8	–	1 ± 1	–	Tr

Note: Errors cited are analyzed uncertainties ($\pm 2\sigma$); Tr = detected in trace amounts (<1%); – = no detection

Location ID	Depth (ft)	Stratigraphic Unit	Smectite	Tridymite	Cristobalite	Quartz	Feldspar	Glass	Hematite	Mica	Hornblende
TA-49	375.0	Qbt 1v	Tr	3 ± 1	17 ± 1	21 ± 2	54 ± 8	–	1 ± 1	–	–
TA-49	385.0	Qbt 1g	–	–	6 ± 2	21 ± 2	45 ± 6	27 ± 6	1 ± 1	–	–
TA-49	395.0	Qbt 1g	–	–	1 ± 1	18 ± 1	29 ± 4	51 ± 4	1 ± 1	–	–
TA-49	405.2	Qbt 1g	–	–	2 ± 1	7 ± 1	20 ± 3	70 ± 3	1 ± 1	–	–
TA-49	419.4	Qbt 1g	–	–	1 ± 1	15 ± 1	24 ± 3	60 ± 3	–	–	–
TA-49	425.8	Qbt 1g	–	–	1 ± 1	15 ± 1	21 ± 3	63 ± 3	–	–	–
TA-49	443.2	Qbt 1g	–	–	1 ± 1	16 ± 1	23 ± 3	60 ± 3	–	–	–
TA-49	458.0	Qbt 1g	–	–	1 ± 1	11 ± 1	17 ± 2	71 ± 2	–	–	–
TA-49	475.0	Qbt 1g	–	–	2 ± 1	36 ± 2	38 ± 5	24 ± 5	–	–	–
TA-49	485.7	Qbt 1g	–	–	1 ± 1	19 ± 1	22 ± 3	58 ± 3	–	–	–
TA-49	496.5	Qbt 1g	–	–	2 ± 1	6 ± 1	13 ± 2	79 ± 2	Tr	–	Tr
TA-49	506.4	Qbt 1g	–	2 ± 1	Tr	16 ± 1	26 ± 4	56 ± 4	–	–	–
TA-49	516.0	Qbt 1g	–	–	1 ± 1	16 ± 1	28 ± 4	55 ± 4	–	–	–
TA-49	529.0	Qbt 1g	–	–	Tr	12 ± 1	34 ± 5	54 ± 5	Tr	–	–
TA-49	539.0	Qbt 1g	–	–	1 ± 1	17 ± 1	22 ± 3	60 ± 3	–	–	–
TA-49	549.0	Qbt 1g	–	–	Tr	14 ± 1	25 ± 4	61 ± 4	–	–	–
TA-49	559.0	Qbt t	–	–	–	8 ± 1	16 ± 2	76 ± 2	–	–	–
TA-49	569.0	Qct	3 ± 1	1 ± 1	1 ± 1	17 ± 1	25 ± 4	53 ± 4	–	Tr	–
TA-49	581.5	Qct	4 ± 1	1 ± 1	1 ± 1	20 ± 2	27 ± 4	46 ± 4	Tr	Tr	–
TA-49	596.0	Qct	2 ± 1	–	3 ± 1	33 ± 2	34 ± 5	28 ± 5	Tr	Tr	–
TA-49	606.5	Qbo	3 ± 1	–	2 ± 1	21 ± 2	24 ± 3	50 ± 3	–	Tr	–
TA-49	615.2	Qbo	3 ± 1	–	2 ± 1	10 ± 1	24 ± 3	60 ± 3	1 ± 1	–	–
TA-49	625.5	Qbo	2 ± 1	–	2 ± 1	11 ± 1	25 ± 4	59 ± 4	1 ± 1	–	–
TA-49	637.2	Qbo	Tr	–	2 ± 1	11 ± 1	24 ± 3	62 ± 3	1 ± 1	–	–
TA-49	647.0	Qbo	2 ± 1	–	2 ± 1	9 ± 1	18 ± 3	69 ± 3	–	–	–
TA-49	656.5	Qbo	2 ± 1	–	2 ± 1	10 ± 1	24 ± 3	61 ± 3	1 ± 1	–	–
TA-49	666.5	Qbo	1 ± 1	–	2 ± 1	11 ± 1	23 ± 3	63 ± 3	–	–	Tr
TA-49	676.5	Qbo	2 ± 1	–	2 ± 1	10 ± 1	22 ± 3	64 ± 3	–	–	–
TA-49	688.0	Qbo	Tr	–	–	4 ± 1	7 ± 1	89 ± 1	–	–	–

This report has been reproduced directly from the best available copy. It is available electronically on the Web (<http://www.doe.gov/bridge>).

Copies are available for sale to U.S. Department of Energy employees and contractors from

Office of Scientific and Technical Information
P.O. Box 62
Oak Ridge, TN 37831
(865) 576-8401

Copies are available for sale to the public from

National Technical Information Service
U.S. Department of Commerce
5285 Port Royal Road
Springfield, VA 22616
(800) 553-6847



Los Alamos NM 87545